Author's reply to 'Interactive comment on "Air-sea gas exchange at hurricane wind speeds" by Kerstin E. Krall and Bernd Jähne' by Byron Blomquist

August 29, 2019

The authors thank Mr. Blomquist for his thorough and helpful comments. A point by point answer to his comments can be found below.

Computation of u_{10}

> Reviewer's comment: However, I would like to see a bit more detail on the assumptions involved in deriving an open ocean-equivalent 10 m wind speed and u* from wind speed measurements in the wind tunnel(p.12).

We now explain this in more detail in the manuscript. To this end we will add our co-workers from Kyoto (Naohisa Takagaki) and Miami (Andrew Smith) as co-authors, because they made the measurements and greatly helped with computing u_{10}. We also found a mistake in converting between $u_{*,a}$ and $u_{*,w}$, and decided to use Donelan et al. (2004) (lab measurements of C_D) instead of Powell et al. (2003) (field measurements of C_D) to convert measured wind speeds in Miami to u_* and u_{10}. This slightly changes the relationships $k_x(u_{*,w})$ and the model parameterization equations, but not our findings. Further details and an in-depth description of the measurement procedure can be found in Takagaki et al. (2012) and Donelan et al. (2004).

Separation of total gas transfer velocity into the components used in Eq. 10.

> Reviewer's comment: I don't fully understand how the parameters defined on p.16 (ks600, kc600 and kr) were obtained from the measurements. Was kc600 determined using only data for SF6 and CF4 (and only SF6 in seawater), as mentioned on p.18 and are these results shown in Fig.7b? Were these then applied as fixed values in a two- parameter fit to data for all gases to obtain ks600 and kr in Fig. 7a,c?

Each wind speed is treated separately. The fit routine does not know u_* or u_{10}. Input parameters are: all k_{meas}, of one wind speed condition, Sc and α calculated at the water temperature k_{meas} was measured at. In a first step, the fit routine minimizes (k_{tot}-k_{meas})^2 using a standard least squares algorithm (`scipy.optimize.curve_fit` in python) where

- k_{meas} is the set of all measured k at one specific wind speed condition, and
- k_{tot} is calculated from the corresponding physico-chemical tracer properties α and Sc using Eqn. 10 with the free and to be optimized parameters k_{c600}, k_{s600} and k_r.

In the next step(s), the condition given by equation 16 is looked at. If it is fulfilled, the fit routine commences and outputs k_{c600}, k_{s600} and k_r from step 1. If the condition Eqn. 16 is not fulfilled, the fit is repeated, however the parameter space is reduced for k_{c600}, with the maximum allowed value of k_{c600} being $k_{c,\text{max}} = k_{meas,T,600} - k_{s600}$ where $k_{\text{meas},T,600}$ is the highest measured, Schmidt number scaled transfer

velocity of either SF_6 or CF_4. This second fit yields a new set of k_{c600}, k_{s600} and k_r, for which the check according to equation 16 is performed again. This is repeated until the condition is satisfied, and the fit routine commences with the results k_{c600}, k_{s600} and k_r from the last iteration step.
This is repeated for each wind speed condition of each of the campaigns separately.
$k_c(\alpha)$-curves as well as plots showing a comparison between k_{meas} and $k_{modeled}$ are shown in the appendix below.

The parameter $k_{c,600}$

> Reviewer's comment: There's potential confusion with the notation for kc600, defined on P.16 as a constant(maximum) value for bubble transfer at a given u*, because kc is also the second term in Eq.10 which could be measured under conditions where Sc=600, but would not be the same as kc600 defined on p.16 since it depends on gas solubility. I suggest using a different notation for the fit parameter representing the maximum limiting value of kc.Perhaps results for kc can also be shown on a plot similar to Fig.2, where the 'kc600' parameter is indicated as the value of kc at the low solubility limit, where the curve is flat?

The definitions are indeed consistent. Maybe this line of reasoning helps:
Starting from Eqn. 9,

$$k_c = \frac{1}{\alpha} k_r \left[1 - \exp\left(-\frac{\alpha}{\alpha_t} \right) \right],$$

assuming that the exponent α/α_t is small, we can calculate the Taylor series up to the second term,

$$\exp\left(-\frac{\alpha}{\alpha_t} \right) = 1 - \frac{\alpha}{\alpha_t}.$$

Inserting this into Eqn. 9 above immediately cancels α, so that k_c indeed does no longer depend on α for small α. Then, replacing α_t with its definition given in Eqn. 8 yields

$$k_{\mathrm{c,low}\,\alpha} = k_{\mathrm{c},600} \left(\frac{600}{\mathrm{Sc}} \right)^{n_b}$$

which is the definition of $k_{c,600}$ in the limit of low solubilities given in Eqn. 6 and also again given on P16. Also have a look at the $k_c(\alpha)$-curves in the appendix below, which show a flattening for the low solubilities. Maybe the confusion comes from the attempt to apply Schmidt number scaling to k_c as given in Eqn. 9 for a gas with a solubility close to, equal or larger than α_t to arrive at something like a CO_2-equivalent bubble surface transfer velocity, which one might also be tempted to also call $k_{c,600}$. However, since k_c as given in Eqn. 9 does depend on the solubility, Schmidt number scaling is not permitted, so that

$$k_c \left(\frac{Sc}{600} \right)^{-n} \neq k_{c,600}$$

for gases with a solubility close to, equal or larger than α_t.

Comparison with other wind-wave tank experiments

> Reviewer's comment: I'm surprised the authors do not present a detailed comparison with results from Rhee et al. 2007, which is a similar wind-wave tank gas transfer study and should be more directly comparable to this work than the field studies.

Rhee et al. (2007) is, among other studies, rather irrelevant for our work, because 1) their highest measured wind speed is 13 m/s, and 2) their means of bubble generation (submerged aerators) is very different from ours (wave breaking induced bubbles only). Therefore such a comparison is not meaningful. In the introduction, we refer, of course, to the two previous lab studies in the Kyoto high wind speed facility: Iwano et al. (2013, 2014) and Krall and Jähne (2014).

Comparison with Mischler's bubble tank experiments and difference between DMS and CO_2

> Reviewer's comment: The absence of detectable bubble transfer below u*w=5.8 m/s for all gases is certainly unexpected, and to me a sign that something is very wrong here. For example, from the information presented in Fig.2 (Mischler, 2014) we expect kc for CO2 (alpha=0.78@ 20°C) and kc for DMS (alpha=12 @ 20°C) to differ by more than a factor of 10.

Figure 1 shows the modeled k_c for DMS and CO_2 in salt water:

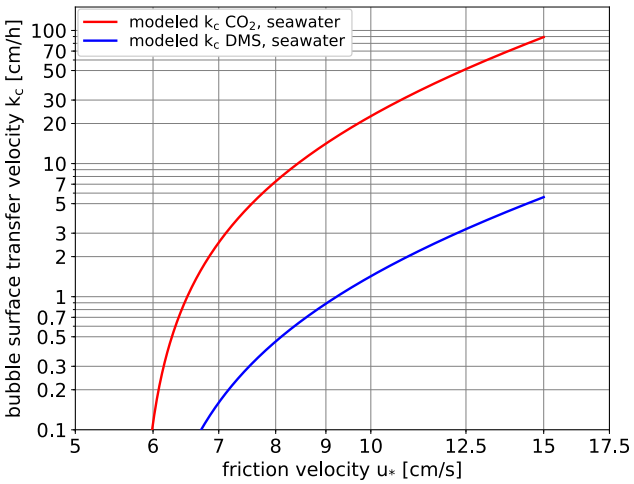

Figure 1: Modeled k_c for DMS and CO_2 in salt water

Both are, as expected, different by more than a factor of 10. However, since k_c for DMS and CO_2 are very small compared to the surface transfer velocity, this difference can hardly be spotted in Fig. 10, where we show the total modeled k of DMS and CO_2. This finding is in perfect agreement with Mischler (2014), who measured pure bubble-induced gas exchange in a special bubble tank.
The reviewer could have easily produced a graph like this for any gas by using the model parameterization equations for $k_{c,600}$ and k_r given in the appendix of the manuscript together with Eqns. 8 and 9 and computed the difference in k_c for DMS and CO_2 for himself.
To summarize, when there are bubble effects, we do indeed see the correct spacing between DMS and CO_2. Nothing is wrong with our data or the fit.

Missing bubble-induced gas exchange at moderatly high wind speeds

> Reviewer's comment: The absence of any difference in transfer rate at moderately high wind speeds among gases covering a broad solubility range is an indication that something is wrong in the determination of kc or that the experimental design is unable to simulate mechanisms of gas transfer at these wind speeds at sea. This result is certainly contradicted by field evidence from several studies showing a generally linear increase in k for DMS at wind speeds of 10-20 m/s and a roughly quadratic increase for a less soluble gas like CO2 over the same interval.

The reviewer's argument is only partially true. Field measurements show a rather confusing picture. While the results of Blomquist et al. (2017) show significantly higher gas transfer velocities for CO_2 than for DMS, the results of Zavarsky (2018) do not (Figure 2). Why is this the case and why are the DMS gas transfer velocities of Blomquist et al. (2017) almost a factor of two lower than those of Zavarsky (2018)? Also, why are gas transfer velocities measured using dual tracer techniques using the very low solubility tracers He and SF_6 (which translates to very large expected bubble contribution) generally much lower than CO_2 transfer velocities measured with eddy covariance (see the compilation of field measurements in Garbe et al. (2014, Fig. 2.10)), even at wind speeds as high as 15 m/s?

Dependency on sea state respectively wave age

> Reviewer's comment: I don't see obvious errors in the theoretical model developed by the authors, which is generally similar to prior treatments in the literature. I suspect the unique conditions in the wind-wave tank at high wind speeds are not comparable to the open ocean. Even an 'infinite fetch' design cannot simulate the wave spectrum in open ocean conditions, except perhaps under light winds, and thus cannot simulate large breaking wave crests and deep bubble plume penetration. I therefore wonder if the absence of bubble-mediated transfer at moderate wind speeds and the observed abrupt jump in the slope of gas transfer at wind speeds above 30 m/s are merely characteristics inherent to the wind- wave tank experimental design?
> I assume high wind interfacial conditions in the tank to correspond to a 'young' sea state, with very high surface stress and widespread coverage with small, choppy breaking waves. This condition is not common at sea except in a situation of very short fetch or a very rapid increase in wind speed, and in any case does not persist long before large breaking waves develop. It's therefore difficult to understand how these results apply to typical 'hurricane wind speed' conditions at sea. The authors should present a detailed analysis of these differences to provide some context for comparisons with field studies.
> *and later ...*
> Nevertheless, at moderate wind speeds of 10-16 m/s sampled under ideal conditions, kco2 from B2017 shows quite a bit of scatter and a high bias compared to other studies, with lower transfer rates observed in 'young' sea states and enhanced transfer in fully developed conditions or in 'old' seas when wind speed is declining but waves are still quite large. These effects are less pronounced for DMS. See Fig.6 in B2017. This implies sea state is a significant factor in the transfer of low solubility gases, and these subtleties are obscured by bin averaging. The comparison between kdms and kco2 likely depends on the specific sea state conditions, and the bubble transfer contribution to low solubility gases in a very 'young' sea state may be significantly reduced, which could be consistent with the kc result in this report.

The authors agree with the reviewer that air-sea gas transfer is not only related to the wind speed, but that the sea state, especially the wave age must be considered as well. But, again, current field results are quite confusing. As the reviewer mentioned, Blomquist et al. (2017) found lower gas transfer velocities in 'young' sea states than in 'old' seas for carbon dioxide and attributed this to higher bubble contributions at older seas. This finding is in strong contrast to estimates of air entrainment due to breaking waves by Deike et al. (2017). They found that the air entrainment is much lower at high wave ages. The effect is large, air entrainment scales roughly with the inverse wave age.
Our short-fetch experiment add results for very young wave ages, where the contribution of bubbles is low again. Therefore currently the issue of wave age dependency needs to be left open. Systematic measurements covering a wide range of wave ages are required.

DMS gas transfer

> Reviewer's comment: DMS is the high-solubility gas in this study (MA was omitted) and should represent interfacial transfer with minimal bubble-mediated contribution. The comparison to data from field studies in Fig.9 looks fairly good to me, despite the fact that there is little or no overlap in the wind speeds. Thus results for the first term in Eq.10, ks, seem roughly consistent with open ocean observations. Instances of suppressed DMS transfer noted in a few field studies are the exception and suggest we don't yet understand all the factors controlling gas transfer emphasis added. The effects of surfactants are an obvious factor that probably suppresses gas transfer, with some support from lab studies, but this has not been carefully examined under field conditions except at low wind speeds. Zavarsky et al. 2018 discuss the possible suppression of transfer by flow separation and angular differences in wind and wave direction.
> With respect to the comparison with results in B2017 (Fig.10 and p.23), I can make a few

clarifications. The B2017 cruise focused on high wind conditions with relatively few flux measurements at U10¡ 8 m/s, and these are generally under non-ideal conditions when the ship was moving at maximum cruise speed to reposition between storm events. So, we expect additional uncertainty or bias in the low wind speed results. Trends shown by the bin averages in Fig.10 are therefore misleading, and in any case the error bars for kdms and kco2 overlap at low wind speeds, so it's not meaningful to say results for the two gases differ by a factor of 3 at U10=3.4 m/s.

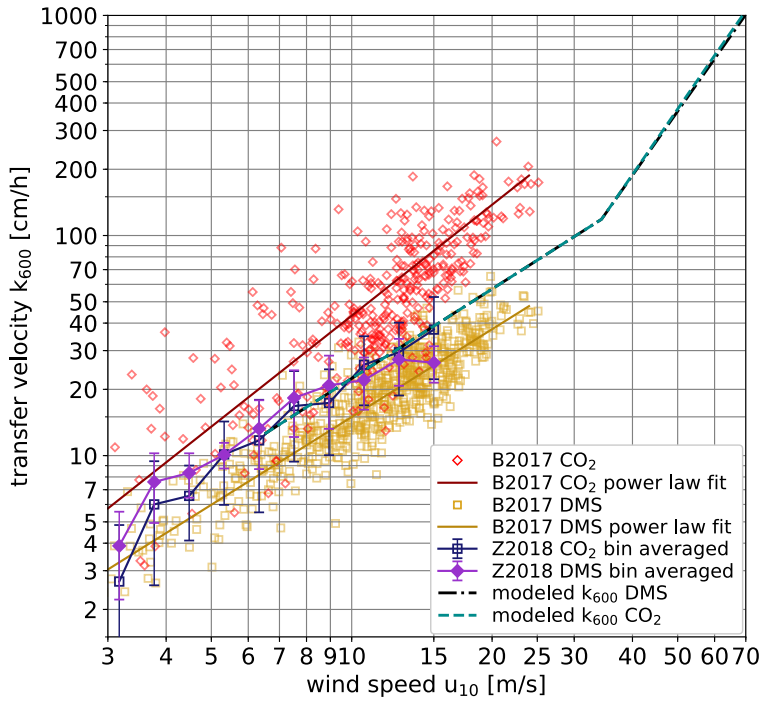

Figure 2: Comparision of DMS and CO_2 gas transfer velocities in a double logarithmic representation: eddy covariance measurements from HiWinGS by Blomquist et al. (2017) (B2017). Also shown are the CO_2 and DMS transfer velocities measured by Zavarsky et al. (2018) (Z2018). The output of the model presented in this paper for CO_2 and DMS is also shown.

We thank the reviewer for this clarification. However, if you plot the individual measurements instead of bin-averaged measurements (Fig. 2), the transfer velocities of carbon dioxide are still significantly higher down to 3 m/s wind speed. We will use then individual measuring points in a revised version of Fig. 10 instead of bin-averaged values, see Fig. 2.

Conclusions

Reviewer's comment: I think this is a carefully conducted study and well written report which explores the mechanisms of gas transfer in a wind-wave tank, but I struggle to understand the significance of these results with respect to conditions in the open ocean, especially at 'hurricane wind speeds'.
I don't agree with the conclusion in Sec.4.6 that rough correspondence between the wave-tank and open ocean data in Fig.11 shows the lab results are capturing the essential mechanisms, since the mechanistic details in each case could be significantly different (the physical details certainly are) and the rough agreement coincidental. As someone with a keen interest in this topic but limited experience with of wind-wave tank experiments I'd like to see a more thorough examination of these issues.

First a comment to the significance of our lab measurements for open ocean conditions. We have done the first systematic study at all in the wind speed range beyond 33 m/s u_{10}. So far only three data points

with huge error bars were available as shown in Figure 11 of our paper. In the wind speed range, we found a very steep increase of the gas transfer velocities even without the effect of bubbles, being associated to various rapid surface fragmentation processes at the free surface. We do not claim that this effect happens in the very same way at the open ocean, but it will happen also there, indicating that also the transfer of all water-side controlled gases will be enhanced significantly. This is an important new finding in our view for the global fluxes between ocean and atmosphere.

It is evident that gas transfer velocity - wind speed relations cannot be transferred from a wind-wave flume to the ocean. This is just as wrong as using empirical gas transfer - wind speed relations from a collection of field experiments. However, we insist that laboratory measurements are invaluable to identify the mechanisms of air-sea gas transfer. Laboratory measurements are generally much more precise and accurate than any current field measuring techniques. It is possible to use much more tracers simultaneously. And it is easy to perform systematic studies. It is not required to perform perfect simulations. This will not be possible. It is just necessary to identify and quantify mechanisms, which can then be adapted to open ocean conditions.

There were two serious limitations in the past: The limited wind speeds and only low-fetch conditions. The first limitation is already gone with the Kyoto High Windspeed Facility and the Miami SUSTAIN Facility. The second one can be overcome in annular facilities such as the Heidelberg Air-Sea Interaction Facility, the Aeolotron (Fig. 3).

Figure 3: Heidelberg Aeolotron: Due to the infinite fetch of the 10 m diameter facility, long and steep breaking wind waves can be generated, much larger than in any linear facility.

We have already modified the Heidelberg Aeolotron to perform experiments at higher wind speeds. With a number of new experimental techniques, which we have started to test this year, we are currently preparing experiments to cover an unprecedented range of wave ages in laboratory experiments and thus hope that we can make a useful contribution to solve the wave age dependency of air-sea gas exchange.

References

Blomquist, B. W., Brumer, S. E., Fairall, C. W., Huebert, B. J., Zappa, C. J., Brooks, I. M., Yang, M., Bariteau, L., Prytherch, J., Hare, J. E., Czerski, H., Matei, A., and Pascal, R. W. (2017). Wind speed and sea state dependencies of air-sea gas transfer: results from the high wind speed gas exchange study (hiwings). *J. Geophys. Res.*, 122:8034–8062.

Deike, L., Lenain, L., and Melville, W. K. (2017). Air entrainment by breaking waves. *Geophys. Res. Lett.*, 44:3779–3787.

Donelan, M., Haus, B., Reul, N., Plant, W., Stiassnie, M., Graber, H., Brown, O., and Saltzman, E. (2004). On the limiting aerodynamic roughness of the ocean in very strong winds. *Geophys. Res. Lett.*, 31(18).

Garbe, C. S., Rutgersson, A., Boutin, J., Delille, B., Fairall, C. W., Gruber, N., Hare, J., Ho, D., Johnson, M., de Leeuw, G., Nightingale, P., Pettersson, H., Piskozub, J., Sahlee, E., Tsai, W., Ward, B., Woolf, D. K., and Zappa, C. (2014). Transfer across the air-sea interface. In Liss, P. S. and Johnson, M. T., editors, *Ocean-Atmosphere Interactions of Gases and Particles*, pages 55–112. Springer.

Iwano, K., Takagaki, N., Kurose, R., and Komori, S. (2013). Mass transfer velocity across the breaking air-water interface at extremely high wind speeds. *Tellus B*, 65:21341.

Iwano, K., Takagaki, N., Kurose, R., and Komori, S. (2014). Erratum: Mass transfer velocity across the breaking air-water interface at extremely high wind speeds. *Tellus B*, 66:25233.

Krall, K. E. and Jähne, B. (2014). First laboratory study of air-sea gas exchange at hurricane wind speeds. *Ocean Sci.*, 10:257–265.

Mischler, W. (2014). *Systematic Measurements of Bubble Induced Gas Exchange for Trace Gases with Low Solubilities*. Dissertation, Institut für Umweltphysik, Fakultät für Physik und Astronomie, Univ. Heidelberg.

Powell, M. D., Vickery, P. J., and Reinhold, T. A. (2003). Reduced drag coefficient for high wind speeds in tropical cyclones. *Nature*, 422:279–283.

Rhee, T., Nightingale, P., Woolf, D., Caulliez, G., Bowyer, P., and Andreae, M. (2007). Influence of energetic wind and waves on gas transfer in a large wind-wave tunnel facility. *J. Geophys. Res.*, 112:5027.

Takagaki, N., Komori, S., Suzuki, N., Iwano, K., Kuramoto, T., Shimada, S., Kurose, R., and Takahashi, K. (2012). Strong correlation between the drag coefficient and the shape of the wind sea spectrum over a broad range of wind speeds. *Geophys. Res. Lett.*, 39.

Zavarsky, A. (2018). *Eddy covariance air-sea gas flux measurements. Regional sources and gas transfer limitation*. PhD thesis.

Zavarsky, A., Goddijn-Murphy, L., Steinhoff, T., and Marandino, C. A. (2018). Bubble-mediated gas transfer and gas transfer suppression of dms and co2. *Journal of Geophysical Research: Atmospheres*, 123(12):6624–6647.

Appendix

The following plots will also appear in a supplement to the final revised paper.

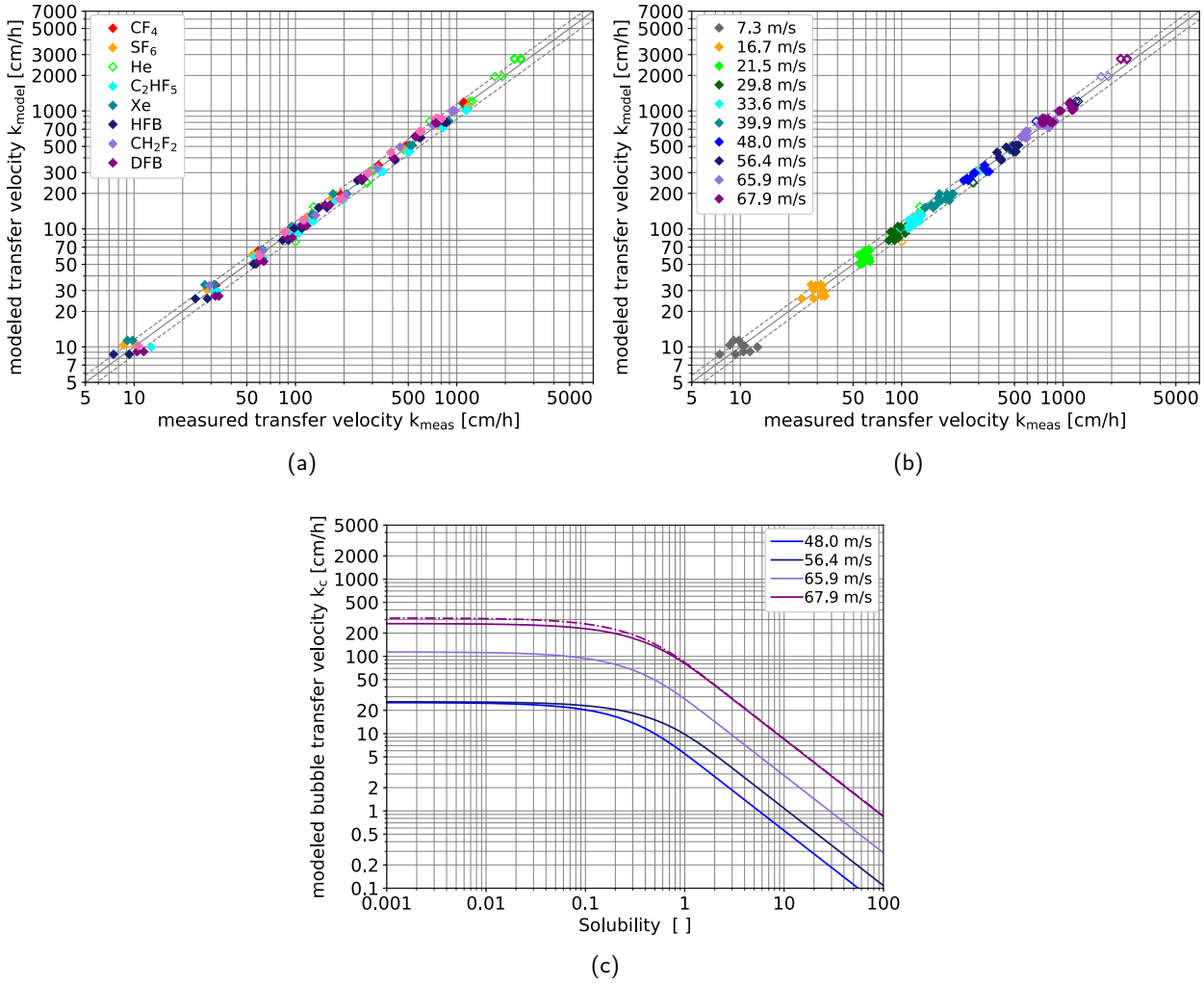

Figure 4: Kyoto freshwater experiment: Modeled vs. measured transfer velocities, colors corresponding to the tracers (a) and colors corresponding to the wind speeds used (b). The solid line marks perfect agreement, the dashed lines plus or minus 15%. He was excluded from the fit, therefore it is only shown here with open symbols. (c) bubble surface transfer velocity k_c in dependency of the solubility for the wind speeds, for which a bubble contribution was detected. The highest wind speed condition was repeated twice, one of the repetitions is shown as a dashed line, the other as a solid line.

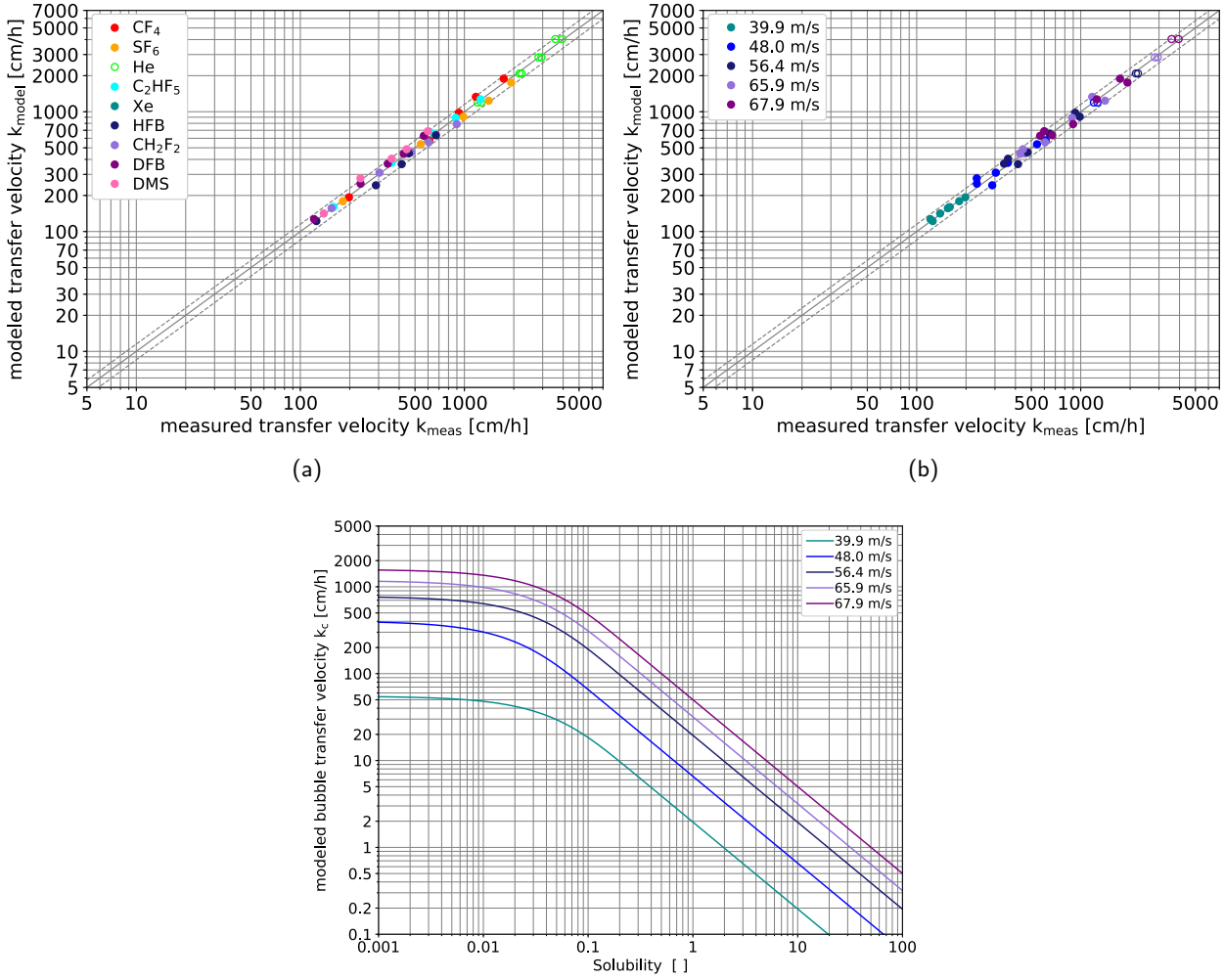

Figure 5: Kyoto seawater model experiment: Modeled vs. measured transfer velocities, colors corresponding to the tracers (a) and colors corresponding to the wind speeds used (b). The solid line marks perfect agreement, the dashed lines plus or minus 15%. He was excluded from the fit, therefore it is only shown here with open symbols. (c) bubble surface transfer velocity k_c in dependency of the solubility for the wind speeds, for which a bubble contribution was detected.

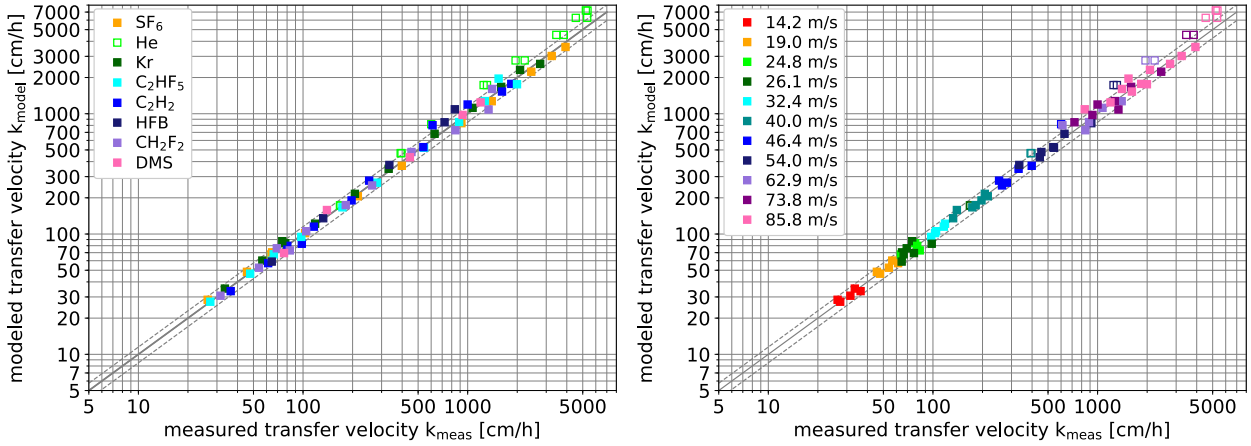

(a) (b)

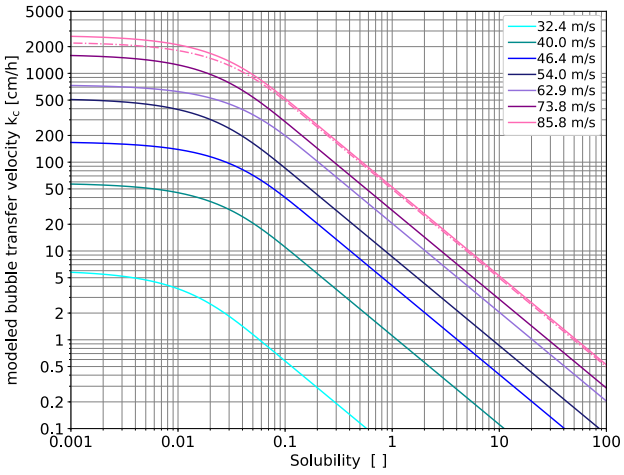

(c)

Figure 6: Miami seawater experiment: Modeled vs. measured transfer velocities, colors corresponding to the tracers (a) and colors corresponding to the wind speeds used (b). The solid line marks perfect agreement, the dashed lines plus or minus 15%. He was excluded from the fit, therefore it is only shown here with open symbols. (c) bubble surface transfer velocity k_c in dependency of the solubility for the wind speeds, for which a bubble contribution was detected. The highest wind speed condition was repeated twice, one of the repetitions is shown as a dashed line, the other as a solid line.

Author's reply to 'Interactive comment on "Air-sea gas exchange at hurricane wind speeds" by Kerstin E. Krall and Bernd Jähne' by Christopher Fairall

September 3, 2019

The authors thank Christopher Fairall for his thorough review and helpful comments. A point by point answer to his questions and comments can be found below.

Missing bubble contribution

> Reviewer's comment: Their main finding – that bubble transfer is negligible compared to the direct transfer for all gases up to wind speeds of 30 m/s – is surprising (at least to this reviewer).

This was very unexpected for the authors as well. This is why we reported the Kyoto results only on conferences but did not write a paper and waited for the results of a second experiment in the much larger SUSTAIN facility with real seawater, where very similar results were obtained.

Reconciliation of lab and field measurements

> Reviewer's comment: The authors' conclusions are difficult to reconcile with open ocean measurements but I leave it to them to consider how to handle that. In my opinion they are too dismissive of the large number of experimental (tracers and eddy covariance) studies that indicate insoluble gases and CO2 have substantially higher transfer velocity above 15 m/s. I question that the Zavarsky paper is sufficient cover.

In the conclusions of our paper, we will put more emphasis on the unsolved problem of wave age or fetch dependency of the gas transfer velocity.
By the way, the authors are surprised that both reviewers do not comment at all our findings for wind speeds beyond 33 m/s, were we found a very steep increase of the gas transfer velocities even without the effect of bubbles, being associated with various rapid surface fragmentation processes at the free surface. We do not claim that this effect happens in the very same way at the open ocean, but it will happen also there, indicating that also the transfer of all water-side controlled gases will be enhanced significantly independently of solubility. In our view, this is an important new finding with relevance for the global fluxes between ocean and atmosphere.

Computation of u_{10} and momentum balance

> Reviewer's comment: I don't understand why they used Powell's open ocean estimates of Cd when they could have used Donelan's 2004 results actually determined in the Miami wind tunnel. Also, please give us a sentence explaining Takagadi's method for getting friction velocity so we don't have to go look it up. I am guessing they assumed a momentum balance at the interface to compute u*w from u*a (square root of ratio of air to water density). This assumes that the growth of the wave field has negligible effect of the momentum balance. Is this right?

Also, they switch back and forth between u*w and just u* - I assume they mean the same thing. Just be advised that it is quite a stretch from a setting on an instrument dial to actual waterside friction velocity.
and later ...
U*a is a measure for momentum extracted from the wind. Some of that momentum is realized in the ocean via direct viscous transfer at the interface, some goes into growing waves and some is later realized as turbulence when waves break. If locally waves are in dynamic balance, then the momentum flux from the air is the same as the momentum flux realized in the ocean. So, how close is the balance in a wind tunnel?

- We now explain this in more detail in the manuscript. To this end we will add our co-workers from Kyoto (Naohisa Takagaki) and Miami (Andrew Smith) as co-authors, because they made the measurements and greatly helped with computing u_{10}. We decided to use Donelan et al. (2004) (lab measurements of C_D) instead of Powell et al. (2003) (field measurements of C_D) to convert measured wind speeds in Miami to $u_{*,a}$ and u_{10} and we also found a mistake in converting between $u_{*,a}$ and $u_{*,w}$, which we corrected for the final paper. This slightly changes the relationships $k_x(u_{*,w})$ and the model parameterization equations, but not our findings.

- In short fetch wind-wave tunnels, the growth of waves has a considerable effect on the momentum balance. At the moment, we have only data from one fetch, measured in the large Marseille facility and only being published in a PhD thesis (Bopp, 2018) with results similar to Banner and Peirson (1998). So the best we could do is to assume momentum balance. We wanted to use the water side friction velocity, because gas transfer is controlled there.

- Indeed, the label in Fig. 5 should read as u_{*w} and not u_* and will be changed in the final paper.

- As a side note, the wind-wave tank that Donelan et al. (2004) used was a different one than the one used in this study (SUSTAIN). So Donelan et al. (2004) did not determine C_d in **the** Miami wind wave tunnel, but merely in **a** Miami wind wave tunnel.

- In the fetch-limited SUSTAIN tank, waves are growing until their structure changes/collapses due to momentum transfer (forcing) from the wind or breaking and they do not reach true equilibrium where air-side and water-side stress are exactly equal. An upcoming experiment in SUSTAIN on the drag coefficient and momentum balance (lab vs. field) is presently in planning stages.

DMS and carbon dioxide

Reviewer's comment: Another example, McNeil and D'Asaro (2007) did not 'measure' gas transfer velocities, they inferred them from water concentration measurements. Furthermore, their basic assumption in the analysis is that both free surface and bubble transfer velocities scale with u*w and nothing else. However, there is considerable evidence that the air volume flux from breaking scales as u* and other wave parameters (see Deike et al. 2017). Also note that Deike and Melville (2018) used this approach to estimate kb for DMS and CO2 – treating both gases as highly soluble. They present measurements of bubble area from the wind tunnels but no estimates of volume flux. I think the bubble volume flux data should appear in Fig. 7c. Finally, the authors might note that Rhee et al. 2007 found considerable enhancement of k for insoluble gases when bubbles were introduced.
and later ...
The discussion of field measurements of k for DMS and CO2 is very useful (Section 4.5). It also illustrates the rather inconclusive state of field observations. The data from Zavarsky et al (2018) show essentially no difference between CO2 and DMS. The analysis of Fairall et al. (2011) which compiled all the direct flux data to date showed significant differences. The HIWINGS data shown in this figure are quite surprising for CO2. Blomquist gives k CO2 a power dependence of u10^1.68, which is not linear. Because of the conditions, I don't think the HIWINGS data below U10 of 10 m/s should be considered. Even ancient information such

as Wanninkhoff's famous formula indicate a quadratic wind speed dependence for insoluble gases. Earlier suggestions that k CO2 should scale as U^3 were based on the assumption that whitecap fraction scaled as U^3. More recent observations have shown that this is not the case, with much weaker wind speed dependence at high wind speeds. I think the authors may be placing too much importance on Zavarsky. From Wanninkhoff's radioactive tracers, to a number of deliberate tracer studies, and perhaps all other eddy flux measurements CO2 goes at least quadratic with wind speed. At u10=18 m/s, the value is close to 100 cm/h for open ocean measurements.

- For the data of McNeil and D'Asaro (2007), we will change 'measured' to 'estimated'.
- We are surprised about the statement that the bubble volume flux V_a should scale linearly with u_*. Did you really mean this? The equations in Fig. 4 in Deike et al. (2017) rather says $V_a = 2.3 \cdot 10^{-3} c_p^{-0.9} u_*^{1.9}$. By the way, this finding is just the opposite of the finding by Blomquist et al. (2017). They found lower gas transfer velocities in 'young' sea states than in 'old' seas for carbon dioxide and attributed this to higher bubble contributions at older seas. Deike et al. (2017) found that the air entrainment is much lower at high wave ages. The effect is large, air entrainment scales roughly with the inverse wave age. Thus the wave age dependency is still an open question and further investigations are required.
- Rhee et al. (2007) is, among other studies, rather irrelevant for our work, because 1) their highest measured wind speed is 13 m/s, and 2) their means of bubble generation (submerged aerators) is very different from ours (wave breaking induced bubbles only). Therefore such a comparison is not meaningful. In the introduction, we refer, of course, to the two previous lab studies in the Kyoto high wind speed facility: Iwano et al. (2013, 2014) and Krall and Jähne (2014).
- We selected the data of Blomquist et al. (2017) because it had the highest wind speeds up to 25 m/s and those of Zavarsky et al. (2018) because they show no difference is the gas exchange rates between DMS and carbon dioxide. We place equal importance to both field studies, and can only state that there are contradicting results. Unfortunately, eddy covariance measurements are still not precise enough (especially compared to gas transfer velocity measurements in the lab) and prone to systematic errors. Our current conclusion is therefore, that there are significant yet unresolved wave age and sea state effects. We will emphasize this more clearly in the conclusions and the abstract of our paper.
- We will add a short paragraph to the manuscript, discussing transfer velocities measured using the dual tracer technique with He and SF_6, which have a very low solubility and should, therefore, have a larger bubble effect than CO_2. However, SF_6 and He were found to have lower transfer velocities than CO_2 measured with eddy covariance, see the compilation of field measurements in Garbe et al. (2014, Fig. 2.10a). This is another contradicting field result.

Minor comments

Reviewer's comment: Bubbles may also suppress turbulence through density stratification.

Correct, but for the wind-wave tanks with just below one meter depth, this effect is not significant at all for our measurements.

Reviewer's comment: Eq (5) This terminology is confusing with the un-numbered equation on Page 2 line 14.

We changed the wording in the first paragraph of Sec. 2.1 for clarity.

Reviewer's comment: Page 4 line 1 Suggest referencing bubble model work of Liang et al. GLOBAL BIO- GEOCHEMICAL CYCLES, VOL. 27, 894–905, doi:10.1002/gbc.20080, 2013 and ear- lier work.

We decided not to cite Liang et al. (2013), because their focus is more on supersaturation and fluxes and they did not measure the transfer velocity.

> Reviewer's comment: Page 5 Eq (7) I am confused by the terminology. Can Qb be volume flux and Qb/As also be a volume flux? If we equate kr with the volume of air ingested per unit area per unit time (units velocity), then that should be on the order of 30 cm/hr at u10=15 m/s and u*w=2 cm/s (see, Deike et al, 2017). That does not compare well with Fig. 7 c, where kr doesn't reach those values until u*w is greater than 10.

- Q_b/A_s has the units of a velocity. We will change its name in accordance with Deike et al. (2017) to 'air entrainment velocity'.
- Deike et al. (2017) found a considerable wave age effect and our measurements add another value for very low wave ages not covered by the data Deike is using.

> Reviewer's comment: Page 5 Eq (10) This equation is similar to Woolf parameterization. For the volume flux is kr=2450*whitecap fraction (cm/h) and the parameter e=kc/kr*sqrt(600). How does this compare to your results?

We can't directly compare because we have not yet estimated the whitecap fraction. We will do this in a further paper once we have analyzed the images from the water surface. Currently, we can only say that the solubility dependency is about the same. However, Mischler (2014) has shown in a bubble tank study, that the Woolf et al. (2007) and the Mischler (2014) parameterizations for the bubble mediated transfer velocity k_c perform equally well, however, the Mischler (2014) parameterization uses one fewer parameter.

> Reviewer's comment: Page 7 section 2.3. This discussion of droplet effects is a little confusing. It seems to me that ejecting a droplet does not change the waterside concentration, so their measurement method does not capture it. If the drop has time, it would transfer gas to the air and that would reduce free surface transfer further down the line. Is that what they are trying to say? This argument about time scales ignores the fact that the droplets leave the wind tunnel before they can do much transferring – this is discussed in Andreas and Mahrt 2016.

Even though the fetch of the wind-wave tanks is rather short compared to open ocean conditions, some of the droplets generated, will impact the water surface again. Andreas et al. (2017) discusses the time scales involved in great detail. They state, that only for the largest radii and for weak winds less than 15 m/s, the droplets fall back into the ocean before they establish equilibrium with the atmospheric gas reservoir. So even though not all spray droplets reimpact the water surface since they are blown out of the wind wave tank, those that do impact the water again do change the water side concentration, since they will have equilibrated with the air.
Since, according to Andreas et al. (2017), at extreme conditions, the spray droplets do come into equilibrium before falling back into the water, the diffusion coefficient of the tracer no longer plays a role in spray mediated gas transfer. Therefore, Helium, despite having a much higher diffusion coefficient than other gases, will no longer have a correspondingly faster transfer velocity across the pray droplet interface, since this transfer velocity only depends on how much spray is generated.

> Reviewer's comment: Figure 10. What drag coefficient is used for the curve shown for modeled DMS and CO2?

We used the u_{10}-$u_{*,w}$ relationship shown as a gray line in Fig. 4a, which corresponds to the drag coefficient shown as the gray line in Fig. 1 below.

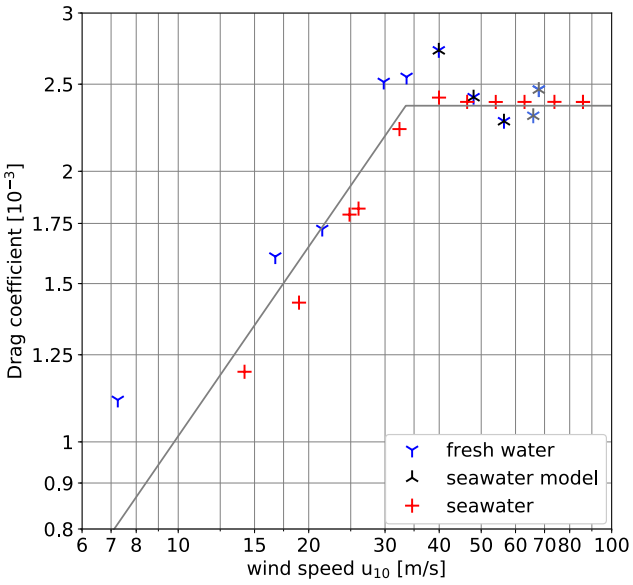

Figure 1: The gray line shows the drag coefficient used for converting $u_{*,w}$ to u_{10} for the Figs. 9, 10 and 11 in the manuscript.

References

Andreas, E. L., Vlahos, P., and Monahan, E. C. (2017). Spray-mediated air-sea gas exchange: the governing time scales. *J. Mar. Sci. Eng.*, 5:60.

Banner, M. L. and Peirson, W. L. (1998). Tangential stress beneath wind-driven air-water interfaces. *J. Fluid Mech.*, 364:115–145.

Blomquist, B. W., Brumer, S. E., Fairall, C. W., Huebert, B. J., Zappa, C. J., Brooks, I. M., Yang, M., Bariteau, L., Prytherch, J., Hare, J. E., Czerski, H., Matei, A., and Pascal, R. W. (2017). Wind speed and sea state dependencies of air-sea gas transfer: results from the high wind speed gas exchange study (hiwings). *J. Geophys. Res.*, 122:8034–8062.

Bopp, M. (2018). *Air-Flow and Stress Partitioning over Wind Waves in a Linear Wind-Wave Facility*. Dissertation, Institut für Umweltphysik, Fakultät für Physik und Astronomie, Univ. Heidelberg, Heidelberg.

Deike, L., Lenain, L., and Melville, W. K. (2017). Air entrainment by breaking waves. *Geophys. Res. Lett.*, 44:3779–3787.

Donelan, M., Haus, B., Reul, N., Plant, W., Stiassnie, M., Graber, H., Brown, O., and Saltzman, E. (2004). On the limiting aerodynamic roughness of the ocean in very strong winds. *Geophys. Res. Lett.*, 31(18).

Garbe, C. S., Rutgersson, A., Boutin, J., Delille, B., Fairall, C. W., Gruber, N., Hare, J., Ho, D., Johnson, M., de Leeuw, G., Nightingale, P., Pettersson, H., Piskozub, J., Sahlee, E., Tsai, W., Ward, B., Woolf, D. K., and Zappa, C. (2014). Transfer across the air-sea interface. In Liss, P. S. and Johnson, M. T., editors, *Ocean-Atmosphere Interactions of Gases and Particles*, pages 55–112. Springer.

Iwano, K., Takagaki, N., Kurose, R., and Komori, S. (2013). Mass transfer velocity across the breaking air-water interface at extremely high wind speeds. *Tellus B*, 65:21341.

Iwano, K., Takagaki, N., Kurose, R., and Komori, S. (2014). Erratum: Mass transfer velocity across the breaking air-water interface at extremely high wind speeds. *Tellus B*, 66:25233.

Krall, K. E. and Jähne, B. (2014). First laboratory study of air-sea gas exchange at hurricane wind speeds. *Ocean Sci.*, 10:257–265.

Liang, J.-H., Deutsch, C., McWilliams, J. C., Baschek, B., Sullivan, P. P., and Chiba, D. (2013). Parameterizing bubble-mediated air-sea gas exchange and its effect on ocean ventilation. *Global Biogeochem. Cycles*, 27(3):894–905.

McNeil, C. and D'Asaro, E. (2007). Parameterization of air sea gas fluxes at extreme wind speeds. *J. Marine Syst.*, 66:110–121.

Mischler, W. (2014). *Systematic Measurements of Bubble Induced Gas Exchange for Trace Gases with Low Solubilities*. Dissertation, Institut für Umweltphysik, Fakultät für Physik und Astronomie, Univ. Heidelberg.

Powell, M. D., Vickery, P. J., and Reinhold, T. A. (2003). Reduced drag coefficient for high wind speeds in tropical cyclones. *Nature*, 422:279–283.

Rhee, T., Nightingale, P., Woolf, D., Caulliez, G., Bowyer, P., and Andreae, M. (2007). Influence of energetic wind and waves on gas transfer in a large wind-wave tunnel facility. *J. Geophys. Res.*, 112:5027.

Woolf, D., Leifer, I., Nightingale, P., Rhee, T., Bowyer, P., Caulliez, G., de Leeuw, G., Larsen, S., Liddicoat, M., Baker, J., and Andreae, M. (2007). Modelling of bubble-mediated gas transfer: Fundamental principles and a laboratory test. *J. Marine Syst.*, 66:71–91.

Zavarsky, A., Goddijn-Murphy, L., Steinhoff, T., and Marandino, C. A. (2018). Bubble-mediated gas transfer and gas transfer suppression of dms and co2. *Journal of Geophysical Research: Atmospheres*, 123(12):6624–6647.

Air-sea gas exchange at ~~hurricane~~ wind speeds up to 85 m s^{-1}

Kerstin E. Krall[1], Andrew W. Smith[2], Naohisa Takagaki[3], and Bernd Jähne[1,4]

[1]Institute of Environmental Physics, Heidelberg University, Im Neuenheimer Feld 229, 69120 Heidelberg, Germany
[2]Rosenstiel School of Marine and Atmospheric Science, University of Miami, Miami, Florida, USA
[3]Department of Mechanical Engineering, University of Hyogo, Himeji 671-2280, Japan
[4]Heidelberg Collaboratory for Image Processing, Heidelberg University, Berliner Straße 43, 69120 Heidelberg, Germany

Correspondence: K. E. Krall (kerstin.krall@iup.uni-heidelberg.de)

Abstract. Gas transfer velocities were measured in two high-speed wind-wave tanks (Kyoto University and the SUSTAIN facility, RSMAS, University of Miami) using fresh water, simulated seawater and seawater for wind speeds between 7 and ~~80~~85 m s^{-1}. Using a mass balance technique, transfer velocities of a total of 12 trace gases were measured, with dimensionless solubilities ranging from 0.005 to 150 and Schmidt numbers between 149 and 1360. This choice of tracers allowed to separate gas transfer across the free interface from gas transfer at closed bubble surfaces. The major effect found was a very steep increase of the gas transfer across the free water surface at wind speeds beyond 33 m s^{-1}~~, which~~. The increase is the same for fresh water, simulated seawater and seawater. ~~This steep increase might start at a lower wind speed in the open ocean as compared to the short-fetch wind-wave tanks.~~ Bubble-induced gas transfer ~~plays~~ played no significant role for all tracers in fresh water and for tracers with moderate solubility such as carbon dioxide and DMS in seawater, while for low solubility tracers bubble-induced gas transfer in seawater was found to be about 1.7 times larger than the transfer at the free water surface at the highest wind speed of ~~80~~85 m s^{-1}. There are indications that the low contributions of bubbles is due to the low wave age / fetch of the wind-wave tank experiments. But further studies on the wave age dependency of gas exchange are required to resolve this issue.

1 Introduction

The transfer of trace gases across the air-sea interface has been an active field of research for almost 40 years (Jähne, 2019). The transfer is characterized by the gas transfer velocity, which depends on environmental forcing such as the wind speed, the amount and strength of wave breaking, the presence of surface active material, number and size of bubbles and spray created by breaking waves (Wanninkhof et al., 2009; Jähne, 2019).

Measuring the gas transfer velocity under hurricane conditions in the field is extremely challenging. Using unmanned floats, McNeil and D'Asaro (2007) managed to ~~measure~~ estimate three gas transfer velocities at wind speeds higher than 25 m s^{-1} during Hurricane Frances in 2004. Due to the difficulties of measuring in the field, wind-wave tanks capable of producing

hurricane force winds are a viable and safe alternative, as they allow for a controlled study of the air-sea interaction mechanisms up to the highest wind speeds.

Until now, only two gas transfer studies have been performed in hurricane conditions in the Kyoto high-speed wind-wave tank with 1,4-difluorobenzene and hexafluorebenzene (Krall and Jähne, 2014) and with carbon dioxide (Iwano et al., 2013, 2014), but only in fresh water. Both studies found a strong increase in the gas transfer velocity at wind speeds higher than approximately 33 to 35 m s^{-1}. Gas transfer was found to increase with more than the third power of the wind speed. However, because of the few gases used, it remains unclear, which process is the main cause of this steep increase. Possible candidates are a) bubbles, which provide an additional surface for the gas transfer, b) an increased water surface area due to the fragmentation of the water surface at highest wind speeds, or c) a strong increase in near surface turbulence due to frequent surface renewal and breakup events, or a combination of all three effects. It is also not clear whether bubble-induced gas exchange differs between fresh water and seawater.

This paper reports the results of extensive gas exchange measurements in two different wind-wave tanks with up to 12 tracers covering a wide range of solubilities using fresh water, simulated seawater and seawater.

2 Air-sea interactions

2.1 Gas Transfer

The flux density j of a trace gas across ~~the~~ a free, smooth or wavy unbroken air-sea interface is governed by the difference in concentration of the gas in air and water (c_a and c_w) and the gas transfer velocity ~~in water~~ k_s across the water surface,

$$j = k_s \Delta c = k_s (c_w - \alpha c_a). \tag{1}$$

Because of the discontinuity at the air-water boundary, the solubility α (here, α is equal to the dimensionless Henry solubility H^{cc} ~~,~~(Sander, 2015)) has to be taken into account. The gas transfer velocity k_s of a sparingly soluble tracer through a free, smooth or wavy, unbroken surface can be described by

$$k_s = \frac{1}{\beta} u_{*,w} \mathrm{Sc}^{-n} \tag{2}$$

(Jähne et al., 1989) with the ~~friction velocity u_*~~ water side friction velocity $u_{*,w}$, a measure for momentum input into the water by the wind, the Schmidt number $\mathrm{Sc} = \nu/D$ of a tracer, given by the ratio of the kinematic viscosity of water ν and the tracer's diffusion coefficient in water D. The dimensionless parameter β and the Schmidt number exponent n depend on the boundary conditions, with $n = 2/3$ for a smooth water surface and $n = 1/2$ for a rough and wavy surface.

From Eq. 2 it is apparent, that the transfer velocities of two sparingly soluble gases A and B can be converted by Schmidt number scaling,

$$\frac{k_{s,A}}{k_{s,B}} = \left(\frac{\mathrm{Sc}_A}{\mathrm{Sc}_B} \right)^{-n}. \tag{3}$$

Commonly, a reference Schmidt number of $\mathrm{Sc} = 600$ is chosen, which corresponds to carbon dioxide at 20^{o}C in fresh water.

For gases ~~,~~that have a medium to high solubility, the transfer resistance in the air side has to be taken into account. As first shown by Liss and Slater (1974) the total transfer velocity k_t can then be expressed by

$$\frac{1}{k_t} = \alpha \frac{1}{k_a} + \frac{1}{k_s} \tag{4}$$

with k_a being the air-side transfer velocity. For gases with a low solubility, the second term dominates and the first term in Eq. 4 can be neglected, such that for those gases $k_t = k_s$. Inverse transfer velocities can be seen as transfer resistances, such that Eq. 4 can be written as

$$R_t = \alpha R_a + R_s. \tag{5}$$

All transfer velocities used in this paper are related to a water side observer, i.~~,~~e., describe how fast a gas in transferred into or out of the water. Air-side observed gas transfer velocities differ by a factor of α.

2.2 Bubble mediated gas transfer

Bubbles contribute to the gas transfer in two ways. First, they provide an additional surface through which gases can pass. Second, during their generation, by rising through the water side mass boundary layer of the water surface, and by bursting at the water surface, they increase the near surface turbulence. Monahan and Spillane (1984) already considered whitecaps as 'low impedance vents', which 'shortcut' the water side transfer resistance. These bubble effects which intensify near surface turbulence increase the transfer velocity across the free surface and do not depend on tracer solubility.

The transfer through a closed bubble surface is different from transfer across the free water surface. First, bubbles have a limited life time, as they either burst at the water surface or, if they are small enough, completely dissolve. Second, bubbles have a limited volume to take up or release gas. Once a bubble is filled to the equilibrium concentration c_b^{eq} given by Henry's law, $c_b^{eq} = \alpha^{-1} c_w$, it is inactive for the remainder of its life time. For gases with higher solubilities and for small bubbles, this equilibrium is reached faster. And third, bubbles experience an overpressure due to hydrostatic pressure and surface tension. Therefore small bubbles can completely dissolve and the equilibrium concentration shifts to slightly higher concentrations. Because the measurements reported here are taken far from equilibrium, dissolving bubbles are not important. The transfer velocities themselves are not affected. A detailed analysis of the time scales involved and how they depend on the bubble radius is given in Jähne et al. (1984).

Because bubbles form an additional exchange surface, the total water side transfer velocity k_w can be split up into two parts (Merlivat and Memery, 1983; Goddijn-Murphy et al., 2016),

$$k_w = k_s + k_c \tag{6}$$

with transfer through the free water **s**urface k_s and through the **c**losed surface of submerged bubbles k_c. It is important to note here that the bubble-induced gas transfer velocity k_c does not include the bubble formation process and the bursting of bubbles when they rise through the surface again. Concerning the gas transfer velocity, these effects cannot be distinguished from other processes generating turbulence close to the water surface, because they do not depend on tracer solubility but only

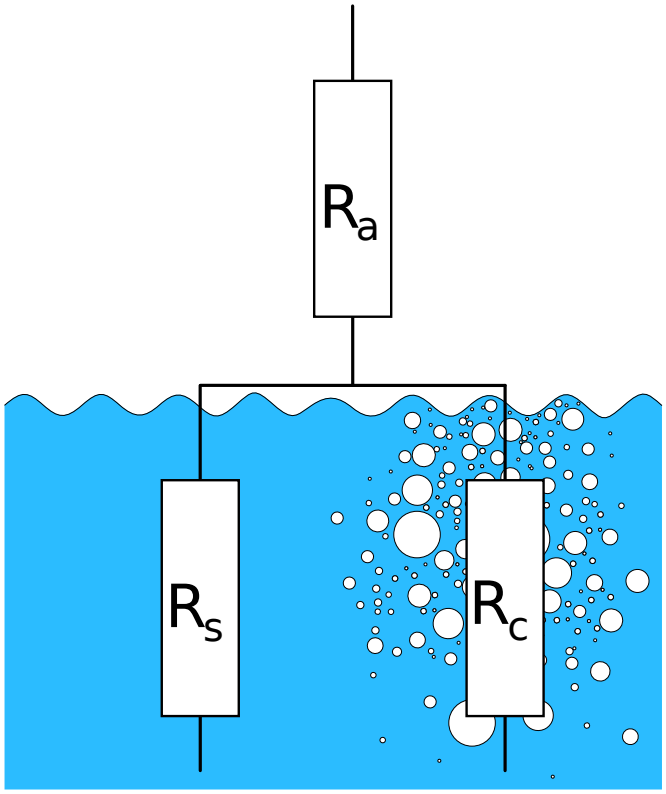

Figure 1. Transfer resistances: R_a: air side transfer resistance, R_s: water side resistance of the free water surface, R_c: transfer resistance of the closed bubble surfaces.

on the Schmidt number. Therefore bubble-induced gas exchange refers here only to the stages in the life time of a bubble with a closed surface and therefore a limited trapped air volume.

Figure 1 shows a schematic view of the resistances for bubble mediated gas transfer $R_c = k_c^{-1}$ in relation to the air and water sided resistances for transfer through the unbroken water surface.

Many approaches have been made to quantify the bubble mediated gas transfer k_c: gas transfer by single bubbles (Maiß, 1986; Patro et al., 2002), transfer in bubble clouds (Asher et al., 1996; Mischler, 2014) and breaking waves (Asher et al., 1995; Leifer and De Leeuw, 2002) as well as theoretical models based on bubble dynamics (Memery and Merlivat, 1985; Woolf and Thorpe, 1991). Bubble mediated gas transfer also depends on bubble surface conditions. It has been shown that surface active material reduces the gas transfer of single bubbles (Maiß, 1986; Patro et al., 2002), while it also decreases the bubbles rise velocity (Alves et al., 2005). During the lifetime of a bubble these surface conditions can change, as bubbles accumulate surface active material while moving through the water.

Empirical or semi-empirical parameterizations (Goddijn-Murphy et al., 2016; Woolf et al., 2007) are state of the art of calculating the bubble mediated gas transfer k_b on the open ocean. Most of these parameterizations link k_b to the tracer's

solubility and Schmidt number (or diffusion coefficient) as well as the whitecap coverage of the water surface, which in turn depends on the sea state that is usually expressed as a function of the wind speed in 10 m height u_{10} or the friction velocity ~~u_*~~ $u_{*,a}$.

Physically based models (Woolf et al., 2007; Mischler, 2014) distinguish two limiting cases, one for very weakly soluble gases and one for more highly soluble ones. For very weakly soluble tracers the bubbles act as a very big reservoir. In that case the bubbles simply provide an additional surface for gas transfer that actively participates in gas transfer for the whole lifetime of a bubble. In this limit, the gas transfer is proportional to the integrated bubble surface area ~~$A_{b,\delta r}$~~ $A_{\mathrm{b},\delta\mathrm{r}}$ per radius interval δr normalized to the water surface area ~~A_s~~ A_s, and the Schmidt number with the bubble Schmidt number exponent ~~n_b~~ n_b, and does not depend on solubility,

$$\begin{aligned} k_{\mathrm{c,low}\,\alpha} \quad k_{\mathrm{c,low}\,\alpha} &= \frac{\int A_{b,\delta r}(r) k_{\mathrm{b},600}(r) dr}{A_s} \quad \frac{\int A_{\mathrm{b},\delta\mathrm{r}}(r) k_{\mathrm{b},600}(r) dr}{A_\mathrm{s}} \left(\frac{600}{\mathrm{Sc}}\right)^{n_b\,\mathrm{b}} \\ &= \qquad\qquad k_{\mathrm{c},600} \left(\frac{600}{\mathrm{Sc}}\right)^{n_b\,\mathrm{b}}. \end{aligned} \tag{7}$$

The transfer velocity k_c is the effective bubble-induced transfer velocity related to the free water surface, while $k_b(r)$ is the real transfer velocity across the bubble surface of a given radius.

In the limit of high solubility, the bubbles constitute a very small reservoir for the trace gas, so that the higher solubility tracers will reach concentration equilibrium $c_b^{eq} = \alpha^{-1} c_w$ very fast. Then the bubble mediated gas transfer can only depend on the tracer's solubility and the total bubble volume flux $Q_{b,\delta r}$ per radius interval δr,

$$k_{\mathrm{c,high}\,\alpha} = \frac{1}{\alpha} \frac{\int Q_{b,\delta r}(r) dr}{A_s} \frac{\int Q_{\mathrm{b},\delta\mathrm{r}}(r) dr}{A_\mathrm{s}} = \frac{1}{\alpha} \frac{Q_b}{A_s} \frac{Q_\mathrm{b}}{A_\mathrm{s}} = \frac{1}{\alpha} k_{r\,\mathrm{r}}. \tag{8}$$

The velocity k_r has an intuitive meaning. It is the effective velocity (volume flux per water surface area) averaged over all bubble sizes, with which the air volume is being submerged by breaking waves and rises towards the surface again. Deike et al. (2017) call this quantity the air entrainment velocity V_a.

The transition solubility, at which the constant bubble mediated transfer velocity for low solubility, $k_{\mathrm{c,low}\,\alpha}$ changes into the transfer velocity decreasing with increasing solubility can be computed by setting both values equal:

$$\alpha_{t\,\mathrm{t}} = \frac{k_r}{k_{\mathrm{c},600}} \frac{k_\mathrm{r}}{k_{\mathrm{c},600}} \left(\frac{\mathrm{Sc}}{600}\right)^{n_b\,\mathrm{b}}. \tag{9}$$

Based on detailed measurements in a bubble-tank with multiple volatile tracers, Mischler (2014) showed that the transition between the two regimes can be well described by a simple exponential term (Fig. 2). The transfer velocity for bubble-mediated gas exchange results in

$$k_{c\,\mathrm{c}} = \frac{1}{\alpha} k_r \frac{k_\mathrm{r}}{\alpha} \left[1 - \exp\left(-\frac{\alpha}{\alpha_t} \frac{\alpha}{\alpha_\mathrm{t}}\right)\right] \approx \begin{cases} k_{\mathrm{c},600} \left(\frac{600}{\mathrm{Sc}}\right)^{n_b} & \alpha \ll \alpha_\mathrm{t} \\ k_\mathrm{r}/\alpha & \alpha \gg \alpha_\mathrm{t}. \end{cases} \tag{10}$$

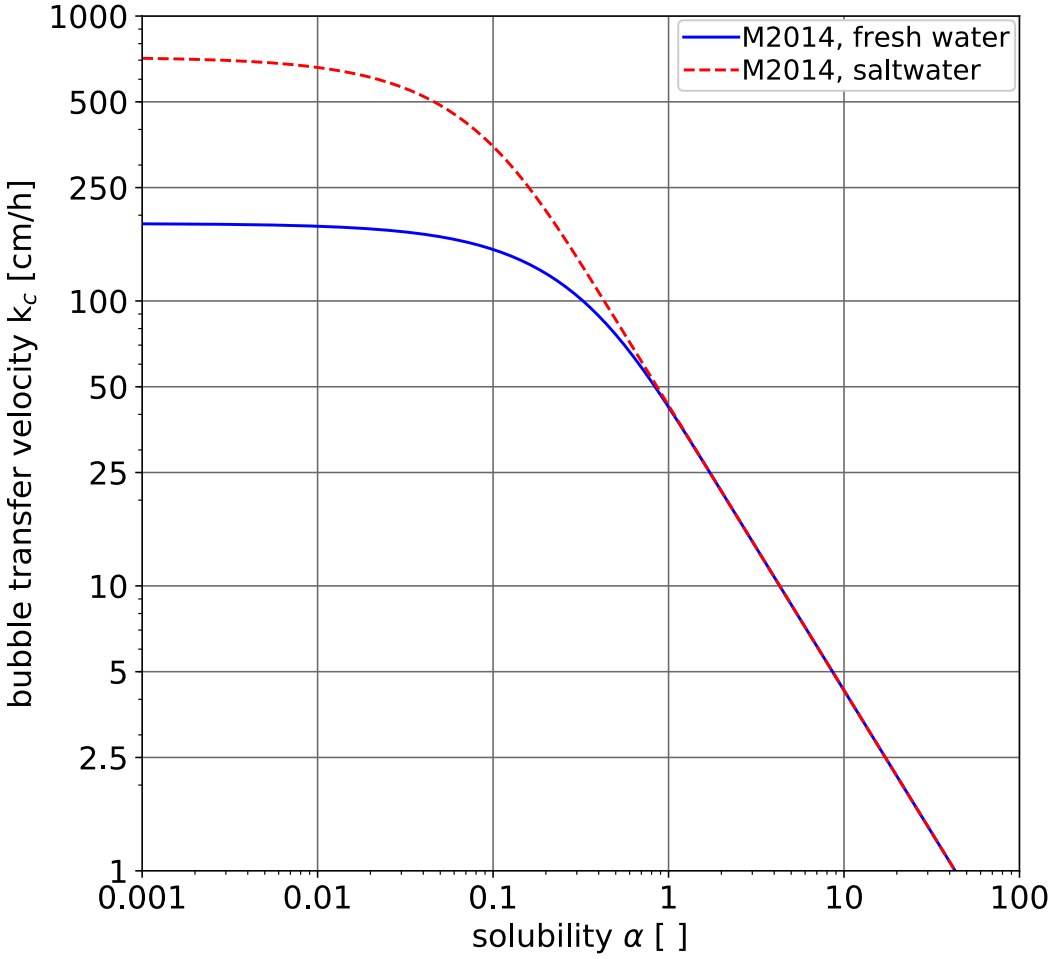

Figure 2. Dependency of bubble mediated gas transfer velocities for the tracers covering a wide range of solubilities as measured in a bubble tank, in which breaking waves were simulated by a water jet for fresh water and seawater (Mischler, 2014). The jet energy was 3.3 W and the bubble volume flux kept constant at about 750 ml min^{-1}, corresponding to $k_r = 43\,\mathrm{cm\,h}^{-1}$.

For fresh water Mischler (2014, Table 9.7) found under the conditions shown in Fig. 2 a transition solubility $\alpha_t = 0.23$ for fresh water and 0.06 for seawater.

In summary, the total gas transfer velocity ~~k_{tot}~~ k_{tot} for water side controlled tracers including bubble-mediated gas transfer can be parameterized as

$$\begin{aligned} k_{\mathrm{tot}} &= k_s \qquad k_{\mathrm{s}} + k_{\mathrm{c}} = k_{\mathrm{s},600}\left(\frac{600}{\mathrm{Sc}}\right)^{0.5} \\ k_{tot} &\\ &+ + \frac{1}{\alpha} k_r \quad \frac{k_{\mathrm{r}}}{\alpha}\left[1 - \exp\left(-\frac{\alpha k_{\mathrm{c},600}}{k_r}\frac{\alpha k_{\mathrm{c},600}}{k_{\mathrm{r}}}\left(\frac{600}{\mathrm{Sc}}\right)^{0.5}\right)\right], \end{aligned} \tag{11}$$

with the three parameters $k_{\mathrm{s},600}$, $k_{\mathrm{c},600}$ and ~~k_r~~ k_{r}. Because the measurements were performed with clean water, the Schmidt number exponents for both the transfer across the free water surface and the bubbles surfaces are set to 1/2. ~~For tracers with a low solubility ($\alpha \ll \alpha_t$)~~In the limits of low and high solubility, the model equation (Eq. 11) ~~can be simplified~~ simplifies to

$$k_{tot} = \begin{cases} (k_{\mathrm{s},600} + k_{\mathrm{c},600})\left(\frac{600}{\mathrm{Sc}}\frac{600}{\mathrm{Sc}}\right)^{0.5} & \alpha \ll \alpha_t \\ k_{\mathrm{s},600}\left(\frac{600}{\mathrm{Sc}}\right)^{0.5} + k_r/\alpha & \alpha \gg \alpha_t. \end{cases} \tag{12}$$

In ~~this case it is possible to simplify the analysis, because~~ the limit of low solubilities, the gas transfer ~~rate~~ velocity does no longer depend on solubility and simple Schmidt number scaling can be applied. The ratio of gas transfer across bubble surfaces and the free surface is then simply given by the ratio of $k_{\mathrm{c},600}$ to $k_{\mathrm{s},600}$.

Whereas in (Eq. 11), a parametric approach is given for the whole solubility range, Deike and Melville (2018, Eq. 12) provide only the high solubility limit in a semi-empiric approach using field DMS and CO_2 gas exchange measurements,

$$k_{tot} = A_{NB} u_{*,a}\left(\frac{600}{\mathrm{Sc}}\right)^{0.5} + \frac{\tilde{A}_B}{\alpha} u_{*,a}^2 c_p, \tag{13}$$

where in the second term $u_{*,a}^{5/3}(gH_s)^{2/3}$ is replaced by the simpler term $u_{*,a}^2 c_p$ using the Toba (1972) relation for fetch-limited waves. The term $\tilde{A}_B u_{*,a}^2 c_p$ is the air entrainment velocity $V_a = k_r$, which, according to Deike and Melville (2018), is *increasing* with the phase speed c_p of the peak wave or its significant weight height H_s, respectively. Surprisingly, Deike et al. (2017) found the air entrainment velocity *decreasing* with the wave age $c_p/u_{*,a}$ by estimating the air entrainment velocity directly, based on a model for a single breaking wave and the statistics of breaking waves as measured in the field.

2.3 Spray mediated gas transfer

The processes mirroring bubbles in the water, spray droplets in the air, is less well studied, with the exception of the transfer of water vapor and heat (Mestayer and Lefauconnier, 1988; Andreas and Emanuel, 2001; Zheng et al., 2008; Jeong et al., 2012; Komori et al., 2018). Only recently, Andreas et al. (2017), evaluated the time scales governing spray-mediated gas transfer for gases other than water vapor in a similar fashion as Jähne et al. (1984) did for bubble-mediated transfer more than three decades earlier.

In contrast to bubbles, tracer solubility plays no role for spray droplets as long as the transfer process is controlled by water-sided processes. This is the case for all tracers used. Therefore spray droplets just constitute an additional exchange surface. The question is only, whether the life time for gas exchange is longer than the life time of the droplets. If this is the case, gas exchange occurs during their whole life time. In this upper limit the gas transfer velocity k_d induced by spray droplet is given in analogy to Eq. 7 by

$$\begin{aligned} k_{\mathrm{d,upper}} &= \frac{\int A_{d,\delta r}(r) k_{\mathrm{d},600}(r) dr}{A_s} \quad \frac{\int A_{d,\delta r}(r) k_{\mathrm{d},600}(r) dr}{A_s} \left(\frac{600}{\mathrm{Sc}} \frac{600}{\mathrm{Sc}}\right)^{n_d} \\ k_{\mathrm{d,upper}} &= \qquad\qquad k_{\mathrm{d},600} \left(\frac{600}{\mathrm{Sc}} \frac{600}{\mathrm{Sc}}\right)^{n_d}. \end{aligned} \tag{14}$$

The transfer velocity k_{d} is the effective droplet-induced transfer velocity related to the free water surface, while $k_d(r)$ is the real transfer velocity across the droplet surface of a given radius.

If the concentration inside the spray droplet equilibrates faster with the surrounding air than the spray droplet takes to fall back into the water, the spray-induced gas transfer velocity k_d depends on the total volume flux Q_d of spray generated (Andreas et al., 2017). This lower limit is given by

$$k_{d,\mathrm{lower}} = Q_d / A_s. \tag{15}$$

At the highest wind speeds, water is lost from wind-wave tanks because the wind tears offs the wave crests and part of the resulting spray droplets leave the facility with the air flow (Sec. 3.2). Therefore the volume lost $\dot{V}_w$ (see Sec. 3.2) is actually a lower limit for Q_d.

Because solubility plays no role for the tracers used in the experiment here, spray-induced gas transfer cannot be distinguished from gas transfer across the free water surface.

Another effect may happen, however. In the limit of a long droplet life time compared to the life time for gas exchange (Eq. 15), the spray droplet induced gas exchange does not depend on the Schmidt number. According to the estimates of Andreas et al. (2017) this is the case, except for largest droplet radii and for weak winds less than 15 m/s. Then, gases with a high diffusivity will no longer show correspondingly higher transfer velocities, if gas transfer through the spray droplet surface is significant.

2.4 Drag coefficient limitation at very high wind speeds

At very high wind speeds, breaking waves disrupt the water surface. It has been shown that the drag coefficient ~~$C_d = u_*^2 u_{10}^{-2}$~~

$$C_d = u_{*,a}^2 u_{10}^{-2} \tag{16}$$

gets saturated or even decreases at wind speeds higher than around $30 - 35\,\mathrm{m\,s^{-1}}$ (Powell et al., 2003; Takagaki et al., 2012; Donelan, 2018). A two phase layer forms, consisting of bubble-filled water transitioning to spray-filled air. The turbulence characteristics of this two phase layer is thought to be controlling the transfer of momentum, which leads to the saturation of

the drag coefficient (Soloviev and Lukas, 2010). However, this does not mean that the friction velocity and thus the momentum input from the wind into the water also decreases, it just increases less steeply.

3 Methods

3.1 The wind-wave tanks

Measurements were performed in two wind wave tanks, the High Speed Wind-Wave Tank of Kyoto University, Kyoto, Japan, in October of 2015 and the SUrge STructure Atmosphere INteraction Facility (SUSTAIN), University of Miami, Miami, USA in May and June of 2017. Table 1 gives an overview of the technical data of the facilities.

Table 1. Technical data of the wind-wave tanks used. All numbers are approximate. The water volume in parentheses for the Kyoto tank gives the total volume when the external tank was used in addition during the highest wind speed condition. Wind speeds and water temperature given in parentheses for the Kyoto experiments is for the seawater model.

	Kyoto Wind-Wave Tank	**SUSTAIN**
water volume [m^3]	8.5(13.7)	120
width [m]	0.8	6
total length [m]	15.7	24
length affected by wind [m]	12.9	18
typical water level [m]	0.75	0.85
air space height [m]	0.85	1.15
water surface area affected by wind [m^2]	10.3	108
wind speeds [$m\,s^{-1}$]	7–67 (41–67)	14–80
water temperature range [^{o}C]	16.0–19.5 (12.8–15)	25.0-27.4
water types	fresh water, simulated seawater	seawater

Water types

Due to technical limitations, seawater could not be used in the Kyoto High Speed Wind-Wave Tank. There, one set of experiments was performed with tap water (referred to as fresh water or FW hereinafter). A second set of experiments was performed in Kyoto with a small amount of n-Butanol added (approx. 700 ml) to the tap water, which modifies the bubble spectrum to better resemble that of seawater (Flothow, 2017). This second set of experiments will be referred to as seawater model ~~or SWM.~~(SWM). The water used in the seawater model will be referred to as simulated seawater.

In the SUSTAIN tank, filtered seawater taken from Biscayne Bay was used. This set of experiments will be abbreviated by SW.

3.2 Mass balances for evasion experiments

A mass balance method is used to measure the gas transfer velocities in evasion type experiments. In this approach, all gases are dissolved in the water and the water is mixed well by pumps, before the wind is turned on. When the wind is turned on, the main flux is from the water volume to the air, and thus the concentration of the tracer in the water c_w decreases exponentially,

$$c_w(t) = c_w(0) \exp\left(-k \cdot \frac{A}{V_w} t\right), \tag{17}$$

with the water volume V_w, the water surface A and the concentration at the start of the experiment $c_w(0)$. In the Kyoto High Speed tank, the water lost due to spray was replaced with fresh water, which changes Eq. 17 to

$$c_w(t) = c_w(0) \exp\left[-\left(k \cdot \frac{A}{V_w} + \frac{\dot{V}_w}{V_w}\right) \cdot t\right], \tag{18}$$

with the water loss rate $\dot{V}_w/V_w$. Thus, knowing the water volume, water surface area and the loss rate and measuring a concentration time series allows to determine the gas transfer velocity k. A more thorough derivation of Eq. 18 can be found in Krall and Jähne (2014).

3.3 Gas concentration measurements, gas handling and tracers

In both experimental campaigns a dual membrane inlet mass spectrometer (HPR-40 MIMS, Hiden Analytical, Warrington, UK) was used to measure the tracers' concentrations in water. The water extracted from the wind-wave tank was pumped along one of the inlet membranes, where dissolved species diffuse through the membrane directly into the vacuum of the spectrometer where they are ionized and subsequently analyzed with respect to their concentrations. For some tracers, two mass to charge ratios were monitored with the MIMS, either because there are sufficiently high concentrations of different Isotopes (e. g. Xe), or the tracer molecule is destroyed in the ionization process and forms multiple ions with a different masses (e. g. DMS, DFB, HFB).

As mentioned in the previous section, before the start of the evasion experiment, all available gases were dissolved in the water and mixed well. For dissolving gases into the water, ~~a membrane contactor~~ membrane contactors (SUSTAIN: Liqui-Cel ~~8x20PVC~~ 8x20 PVC, Kyoto: Liqui-Cel 4x13, Membrana 3M, Charlotte, NC, USA) ~~was~~ were used. In Miami, the gases were dissolved directly into the water of the wind-wave tank, while in Kyoto the gases were first dissolved into a holding tank of approx. 7 m^3. This water was then mixed into the main water volume of the wind-wave tank using pumps before the start of an experiment. Care was taken that the tracers were mixed into the water as homogeneously as possible. To achieve this, the pumps were kept on even after gas loading was finished, and the concentration was monitored. Only when the concentration was sufficiently stable the pumps were turned off and the experiment was started.

The tracers were chosen in this study to cover a wide range of solubilities and Schmidt numbers. Table 2 gives an overview of the tracers used sorted by their solubility. Due to technical and logistical reasons, not all tracers could be used in both facilities. Figure 3 shows the tracers in a Schmidt number–solubility diagram for all conditions encountered. The temperature dependency of the solubility and Schmidt number is apparent. Also shown is for which solubility-Schmidt number combination

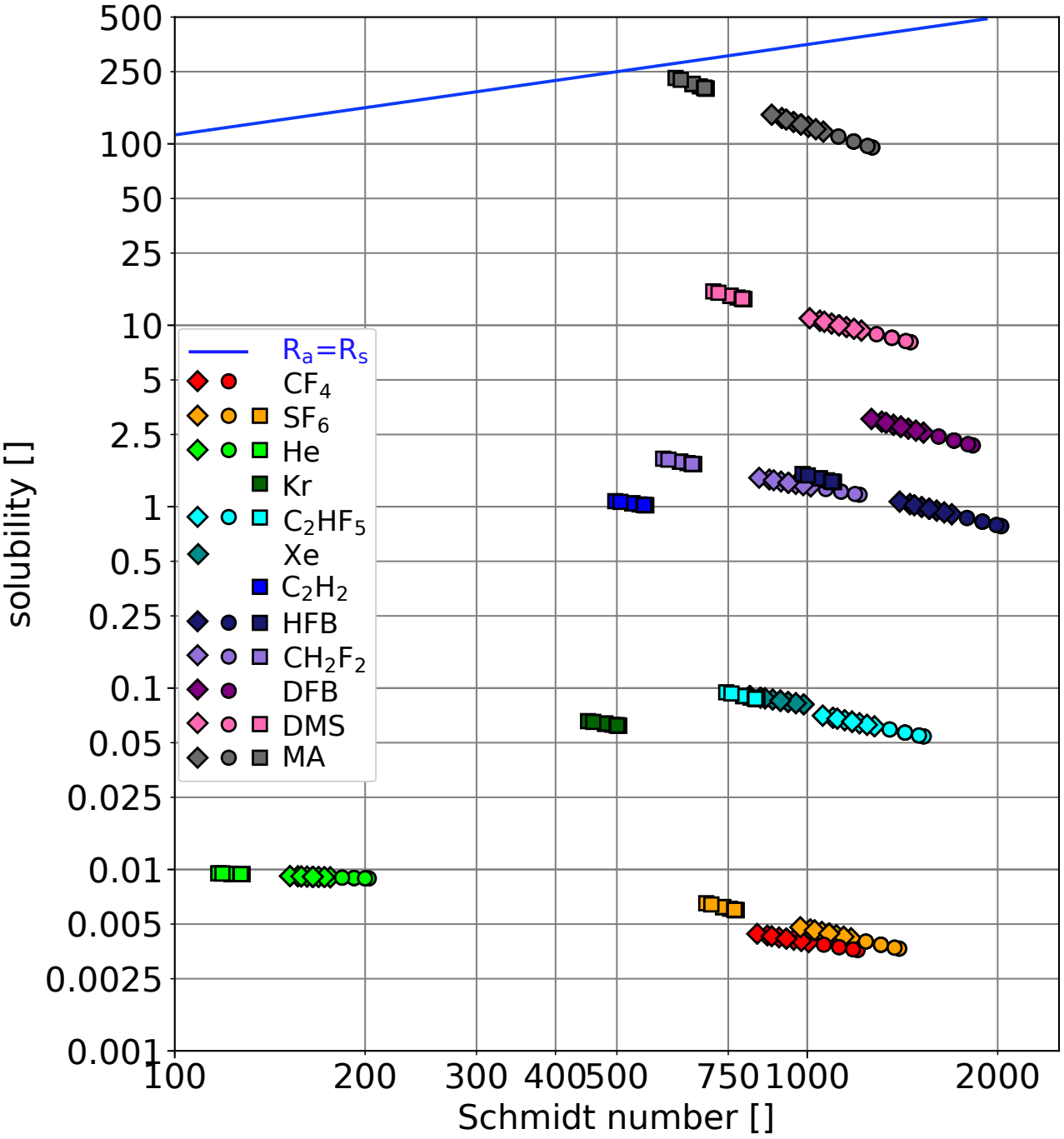

Figure 3. Schmidt number - solubility diagram of the tracers used in this study. Also shown as a blue line is for which solubility the air side resistance is equal to the water side resistance (Eq. 5 for a rough water surface). Diamonds: fresh water (Kyoto), circles: seawater model (Kyoto), squares: seawater (Miami). The variations in the Schmidt number and solubility result from the varying water temperatures used in the different experiments, see Table 1.

the air side resistance equals the water side resistance ($\alpha R_a = R_s$, see also Eq. 5). To calculate the resistances, a rough and wavy water surface was assumed (i. e. $n = 1/2$). Below this $\alpha R_a = R_s$ line, the water side resistance dominates, therefore, the tracers are called water side controlled tracers. All tracers used in this study can be classified as water side controlled tracers, with the exception of Methylacetate (MA), which is partially air side controlled due to its relatively high solubility.

Table 2. Tracers used in this study. PFE: C_2HF_5, HFB: hexafluorobenzene, DFB: 1,4-difluorobenzene, DMS: dimethyl sulfide, MA: methyl acetate. Solubility and Schmidt number are given at 20^oC for fresh water. Schmidt numbers were calculated from the kinematic viscosity (Kestin et al., 1978) and the diffusion coefficient given in the respective citation. ($^{(*)}$ measured only in seawater. $^{(\dagger)}$ measured only in fresh water. $^{(\ddagger)}$ measured only in fresh water and seawater model.)

Tracer	Solubility	Schmidt number
$CF_4{}^{(\ddagger)}$	0.0045^a	812^h
SF_6	0.0049^a	950^i
He	0.0092^b	149^j
$Kr^{(*)}$	0.055^b	624^j
PFE	0.072^c	1030^h
$Xe^{(\dagger)}$	0.092^b	789^j
$C_2H_2{}^{(*)}$	0.91^d	686^h
HFB	1.1^e	1360^h
CH_2F_2	1.5^f	818^h
$DFB^{(\ddagger)}$	3.1^e	1230^h
DMS	11.2^a	983^h
MA	150^g	856^h

[a](Warneck and Williams, 2012); [b](Abraham and Matteoli, 1988); [c](Reichl, 1995); [d](Sander et al., 2011); [e](Hiatt, 2013); [f](Maaßen, 1995);[g](Fenclová et al., 2014); [h](Yaws, 2014); [i](King and Saltzman, 1995); [j](Jähne et al., 1987)

3.4 Wind speed measurements

Kyoto experiments

In the Kyoto tank, wind speeds were not recorded during the experiments. In Takagaki et al. (2012)~~describes the measurements of the reference wind speed in 10m height u_{10} and of the friction velocity u_* in the Kyoto Tank.~~, streamwise and vertical air-side velocity fluctuations, measured using a laser Doppler anemometer and phase Doppler anemometer (LDA and PDA, Dantec Dynamics, Denmark) at a fetch of 6.5 m in the Kyoto tank are given. They estimated the friction velocity $u_{*,a}$ by the Reynolds stress. Special care was taken that neither spray droplets, nor the water film adhering to the side walls of the tank adversely affected the measurements (see also Komori et al. (2018)).

Since we used the same wind generator settings as Takagaki et al. (2012) wind speed and friction velocities were taken from there ~~.~~with the exception of $u_{*,a}$ at the two highest wind speed settings. In Takagaki et al. (2012), $u_{*,a}$ at the highest wind generator setting (fan rotation number 800 rpm) was found to be smaller than $u_{*,a}$ at the second highest wind generator setting (fan rotation number 700 rpm), which might be due to a large measurement uncertainty owing to intensive wave breaking. These values were extrapolated using a polynomial fit to the data reported in Takagaki et al. (2012), such that $u_{*,a}$ used here is strictly monotonically increasing with the wind speed setting as expected. These values of the friction velocity $u_{*,a}$ together with the wind speed values u_{10} taken unaltered from Takagaki et al. (2012) were used to calculate the drag coefficient.

SUSTAIN experiments

A 3D sonic anemometer (IRGASON, Campbell Scientific Inc., Logan, USA) was mounted in the test section of the SUSTAIN wind wave tank at a fetch of 0.65 m and a height of 1.79 m above the tank bottom. The measured wind speeds were converted to the friction velocity ~~u_*~~ $u_{*,a}$ and the wind speed ~~u_{10}~~ u_{10} using the parameterization for the Drag coefficient ~~and the roughness length given in~~ given in Donelan et al. (2004) with the assumption of a logarithmic wind profile. Wind speed uncertainty was calculated from the device uncertainty as specified by the manufacturer as well as the variance of the wind speeds measured. Uncertainties found were in the order of 3 to 4%.

3.5 Bubble measurements

Bubble size distributions were measured in Kyoto using an optical bright field imaging technique (Mischler and Jähne, 2012; Flothow, 2017). ~~In this method, a camera~~ A Nikon D800 digital SLR camera with a 200mm f/4 AF-D macro lens looks perpendicular to the wind direction through the water into a purpose built LED light source. Bubbles entrained in the water scatter the light such that the light no longer reaches the camera sensor, and the bubble appears as a dark circle. Out of focus bubbles have a blurry edge, which is used to estimate the 3D volume the bubbles are in in the 2D images taken by the camera ~~(~~by depth from focus ~~)~~(Jähne and Geißler, 1994). Two bubble imaging systems ~~consisting of a Nikon D800 digital single lens reflex camera and a purpose built LED light source each~~ were operated during the measurements in Kyoto, one at a fetch of 3 m, the second one at 8 m fetch, approximately 30 cm below the water surface. Calibration and data evaluation is described in detail in Flothow (2017).

4 Results

4.1 Wind speeds and friction velocities

The relationship between the water sided friction velocities $u_{*,\mathrm{w}}$ and the wind speeds in 10 m height, u_{10} at which the gas transfer velocities were measured in this study is shown in Fig. 4a. A clear change in the steepness of the relationship can be seen at a wind speed of approximately 33 m s^{-1} as indicated by the gray line. The wind speed of 33 m s^{-1} corresponds to a

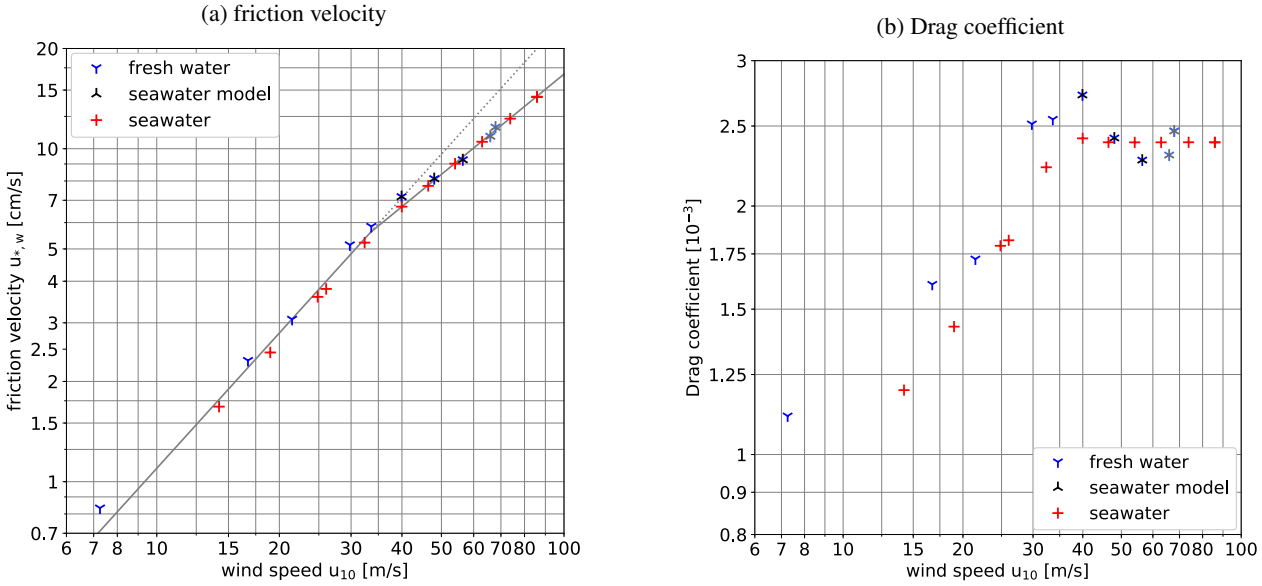

Figure 4. Relationship between the wind speed in 10 m height, u_{10}, and the water side friction velocity (a) and the Drag coefficient calculated using Eqn. 16 (b). Lighter colors mark conditions, where the friction velocity was approximated, see Sec. 3.4.

friction velocity of about 6 cm s^{-1}. Also, the Drag coefficient C_{D} (Fig. 4b) has a maximum at this wind speed, before it levels off.

4.2 Bubble surface area

Up to now, bubble measurements were evaluated only for the Kyoto facility. From the bubble concentration measurements, the total bubble surface was computed and plotted in Fig. 5 as a dimensionless area in relation to the flat free water surface area, A_b/A_s. The uncertainties are quite high, because bubbles where measured only at one depth (Sec. 3.5). But still a few important findings can be stated.

1. The bubble surface area strongly increases with the friction velocity ($\propto u_{*,\mathrm{w}}^3$ to $\propto u_{*,\mathrm{w}}^4$) in all facilities and for fresh water and seawater.

2. For fresh water the bubble surface area almost reaches the same area as the flat free surface at the highest wind speeds.

3. In the modeled seawater the bubble surface area is about ~~on~~ an order of magnitude ~~higher~~ larger than in fresh water. At higher friction velocities, especially with the seawater model, the bubble clouds get very dense, resulting in a systematic underestimation of the bubble surface area. Therefore the true bubble surface area at the highest wind speed is very likely larger than the measured surface area of about four times the area of the flat free water surface.

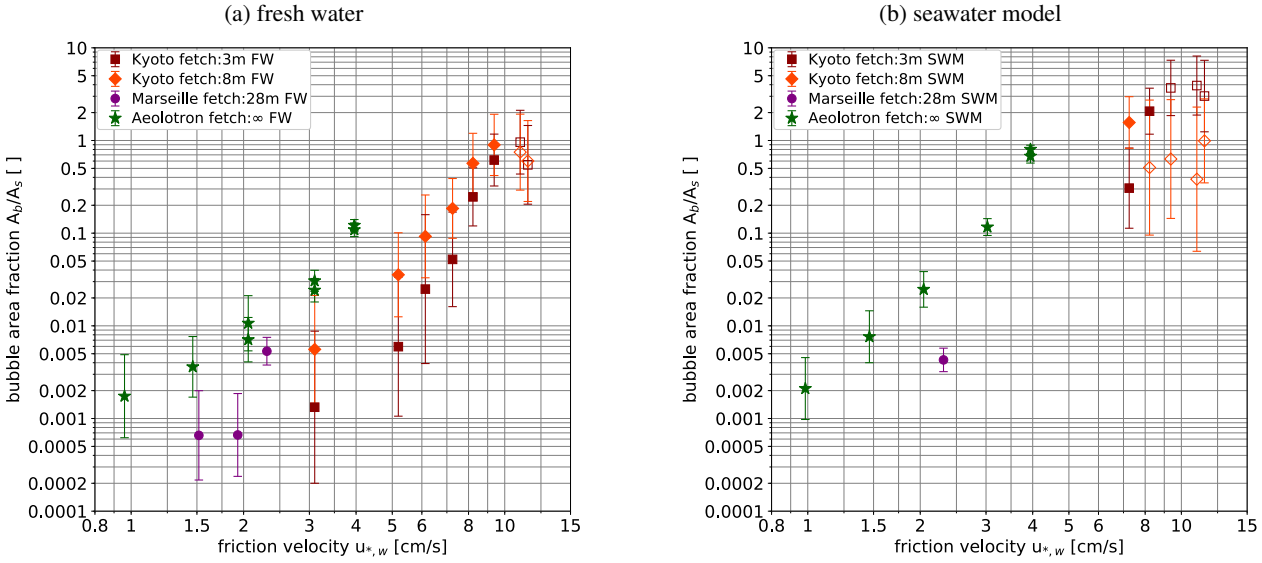

Figure 5. Bubble surface area per water surface area measured in fresh water (a) and seawater modeled by adding butanol to fresh water (b): Kyoto: 3 and 8 m fetch, camera installed approx. 30 cm below water surface at rest; Marseille Luminy: 28 m fetch, camera installed at approx. 50 cm below water surface at rest; Aeolotron Heidelberg: infinite fetch, camera installed at 10 evenly spaced positions between 0.5 and 36.5 cm below the water surface. At the highest wind speeds, the density of the bubbles is so large that the intensity of the illumination that reaches the camera reduces by up to 75 %, which leads to a systematic underestimation of the bubble surface area. Conditions likely affected by this are marked with an open symbol. Figure reproduced from data by Flothow (2017).

4. The bubble surface area shows a clear trend to increase with fetch. Also shown in Fig. 5 are measurements performed at 28 m fetch (Marseille tank), and quasi infinite fetch in the annular wind-wave facility, the Heidelberg Aeolotron in addition to the measurements in Kyoto at 3 and 8 m fetch. Roughly, the same bubble surface area is obtained at about half the friction velocity in the Aeolotron as compared to 3 m fetch in the Kyoto facility. With the modeled sea water the bubble surface area becomes equal to the flat free surface area at a friction velocity just above 4 cm s^{-1}, while this value is reached in the Kyoto facility only at a friction velocity of about 8 cm s^{-1}. This finding is important when extrapolating laboratory results to the field and will be discussed further in Sec. ??4.5.1.

4.3 Measured gas transfer velocities

Figure 6 shows the measured gas transfer velocities k_{meas} in dependency of the water-sided friction velocity $u_{*,\mathrm{w}}$ for three different measurement conditions: (a) fresh water in Kyoto, (b) seawater model in Kyoto and (c) seawater in Miami. Gas transfer increases strongly with the wind speed for all tracers. Beyond a friction velocity of approx. 6 cm s^{-1}, the increase is significantly steeper.

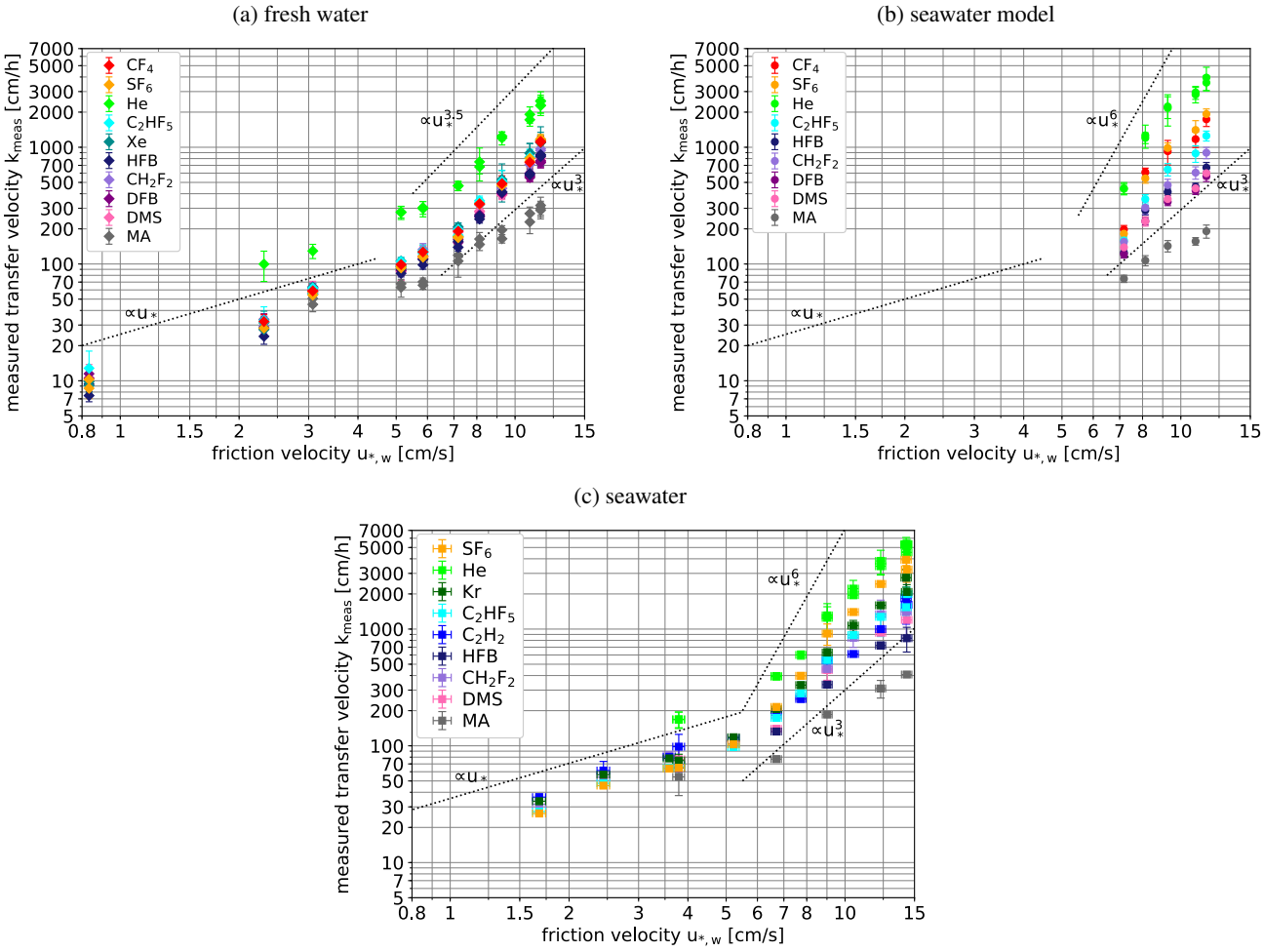

Figure 6. Measured gas transfer velocities k_{meas} in fresh water in Kyoto (a), in the seawater model in Kyoto (b) and in seawater in Miami (c) and (d). Tracers in the legend are sorted by increasing solubility. As a visual guide, lines showing exponential proportionalities between the transfer velocity and the friction velocities to varying powers are shown.

The tracer with the highest solubility, Methylacetate (MA), shows a transfer velocity significantly lower than for the other tracers for all wind speeds and all water types. This reduction in the gas transfer velocity confirms the existence of an additional air side resistance for this tracer, see Sec 2.1. Due to this additional air side resistance, MA will be excluded in the following discussion. From Fig. 6 it is also evident that He has a much higher transfer velocity than the other tracers for all wind speeds. This is caused by its significantly higher diffusion coefficient corresponding to a low Schmidt number, while all other tracers vary in the Schmidt number by at most a factor of two, see Table 2.

Figure 6 also shows dependencies of the form $k_{\mathrm{meas}} \propto u_{*,\mathrm{w}}^{x}$ with a variable exponent x. Clearly, the functional dependency between k_{meas} and $u_{*,\mathrm{w}}$ dramatically changes at a friction velocity of around 6 cm s^{-1}, indicating a new regime starting at this friction velocity. This finding is in good agreement with the earlier measurements of Iwano et al. (2013) and Krall and Jähne (2014), who also found a transition to a much steeper increase at 33 - 35 m s^{-1} (u_{10}). Also, this wind speed coincides with the change in the ~~$u_*(u_{10})$~~ $u_{*,w}(u_{10})$ relationship discussed in section 4.1.

A closer look at the fresh water transfer velocities (Fig. 6a) reveals an unexpected result. Even for high wind speeds all tracers (except He and MA) have transfer velocities within a very narrow band, even though their solubility differs by several orders of magnitude. This is a clear indication, that transfer through closed bubble surfaces is much slower than the transfer through the water surface for fresh water even at the highest wind speeds.

In seawater and in simulated seawater (Figs. 6b and 6c), a clear spacing between the transfer velocities of tracers with different solubilities at high wind speeds can be seen. This means that bubble-induced gas transfer does play a role for seawater.

4.4 Separation of gas transfer across the free surface and bubbles

Once bubbles influence air-sea gas transfer, a separation of the different contributing mechanisms is required. Because of the additional influence of solubility, it is not possible to simply apply Schmidt number scaling. This is why the model combining gas transfer across the free water surface and bubble surface was developed in Sec. 2.2, see Eq. 11. Because all measurements were made at high wind speeds with clean water, the Schmidt number exponent was fixed to 0.5. Then, three unknown parameters remain for each measuring condition:

- The transfer velocity across the free water surface at a Schmidt number of 600, $k_{\mathrm{s},600}$
- The limiting or maximum transfer velocity across the closed-bubble surfaces at a Schmidt number of 600, $k_{\mathrm{c},600}$. It is reached for gases with a solubility $\alpha \ll \alpha_t$.
- The transfer velocity associated with the bubble volume flux ~~per water surface area~~density, k_{r}. ~~In the limit of high solubilities~~ For high solubility ($\alpha \gg \alpha_t$) the bubble-mediated gas transfer velocity is k_{r}/α, compare Eq. 8.

Because of the multi-tracer approach with more than three tracers covering a wide range of solubilities, it is possible to retrieve all three parameters of the model (Eq. 11) for each measuring condition separately and thus to separate the gas transfer across the free water surface from the bubble-induced gas transfer. In addition the transition solubility α_t can be computed according to Eq. 9. The model equation 11 was fitted to the data using a least squares algorithm with the free parameters

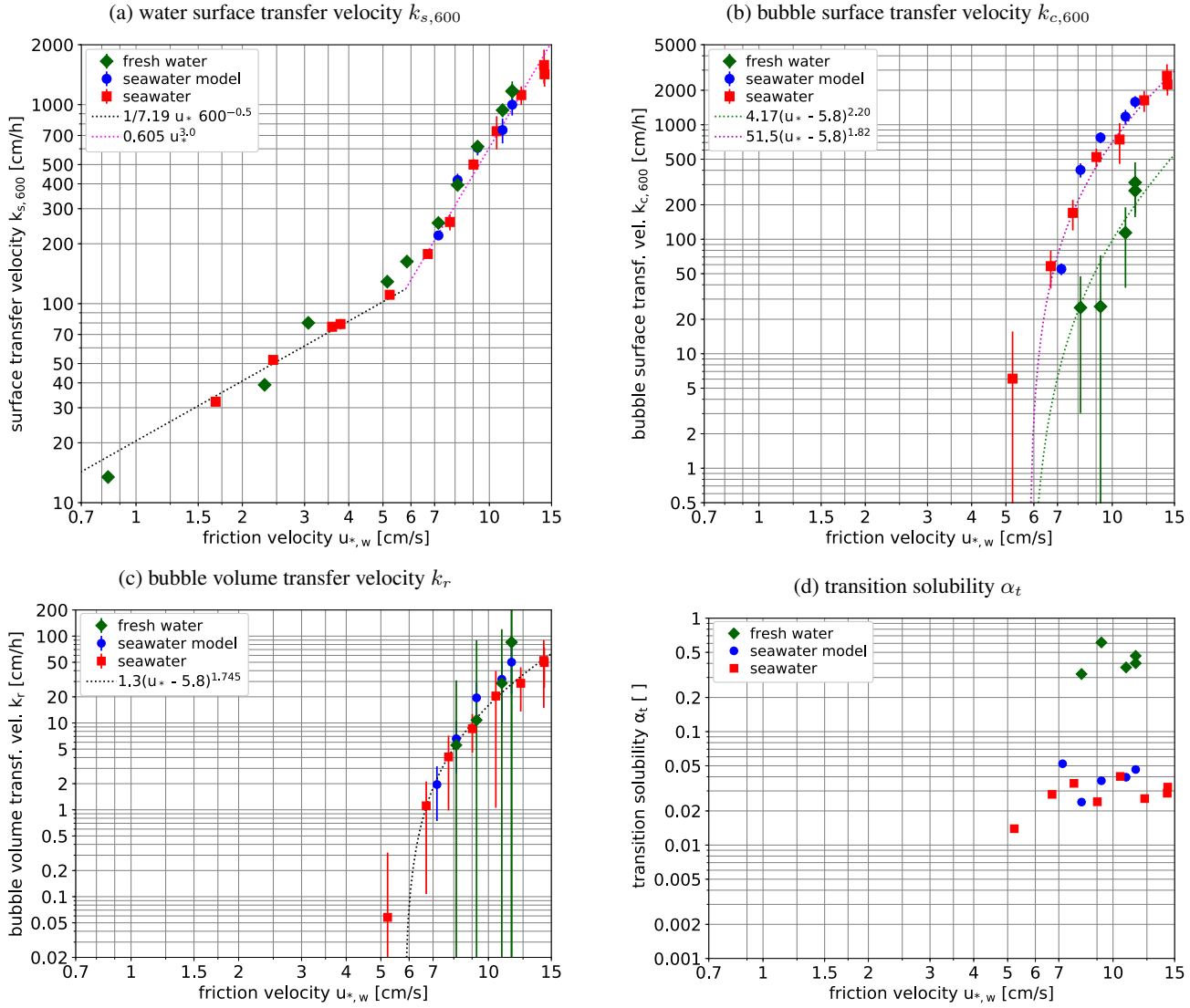

Figure 7. Fitted contribution of the different components to the gas transfer velocity: a) surface transfer velocity $k_{s,600}$, b) bubble surface transfer velocity $k_{c,600}$, and c) the bubble volume k_r as a function of the water side friction velocity in double-logarithmic presentation. Please note the different vertical scales. The graphs include error bars of the fitted parameters. In addition the transition solubility α_t computed according to Eq. 9 in shown in figure d) without error bars.

$k_{s,600}$, k_r and $k_{c,600}$. MA was excluded from the fit due to its additional air side resistance. Also, He had to be excluded. Including He led to unrealistically low transition solubility of below 0.001. One possible reason for this is the high diffusion coefficient of He, and the resulting fast gas transfer from water into the bubbles, which might deplete the He concentration in the water between the bubbles inside bubble clouds. This effect has been observed and described before by Woolf et al. (2007).

Another explanation is spray-induced gas transfer, which could limit the gas transfer velocity of tracers with high diffusivity as discussed in Sec. 2.3.

Also, as a further quality criterion, the fit was required to obey

$$k_{c,600} \leq k_{\mathrm{meas,T}} \left(\frac{Sc_T}{600} \right)^{0.5} - k_{s,600} \tag{19}$$

~~by limiting the available parameter space of $k_{c,600}$ for~~ for the tracers ~~T with solubilities smaller than 0.01 and Schmidt numbers larger than 300 (i.e. for the tracers T=[SF_6 and ,CF_4).]~~. This was achieved by iteratively narrowing the allowed parameter space of the parameter $k_{c,600}$. Eq. 19 describes the highest physically reasonable $k_{c,600}$ (see also Eq. 12). At each measuring condition, the regression with three free parameters was performed with 5–14 measured transfer velocities. For some tracers, the concentrations of two different ions of the same tracer were analyzed with the MIMS, which allowed the measurement of two transfer velocities per tracer for a single wind speed condition, see Sec. 3.3.

The mean (median) deviation between the measured and the modeled transfer velocity is 7.4 % (6.3 %) of the measured transfer velocity. Out of a total of 242 pairs of measured and modeled values, only 22 deviate by more than 15 %. The maximum deviation found was 31.2 % (Acetylene in seawater at ~~$u_{10} = 58.6$~~$u_{10} = 62.9\,\mathrm{m\,s^{-1}}$). This indicates that the regression model is in good agreement with the measured data.

Figure 7 shows the resulting fitted parameters $k_{\mathrm{s},600}$, k_r and $k_{\mathrm{c},600}$ and the calculated transition solubility α_t (see Eq. 9). The bubble-related parameters k_r and $k_{\mathrm{c},600}$ are found to be zero for friction velocities below $5.8\,\mathrm{cm\,s^{-1}}$ for fresh water and seawater. No experiments below $7\,\mathrm{cm\,s^{-1}}$ were performed for the seawater model. The separation of the gas transfer velocity into its different components gives a detailed insight into the mechanisms of air-sea gas transfer at high wind speeds with unexpected results:

Free surface transfer, $k_{s,600}$: The gas transfer velocity across the free water surface $k_{\mathrm{s},600}$ normalized to a Schmidt number of 600 (Fig. 7(a)) clearly shows a transition to a much steeper increase of the transfer velocity with the friction velocity from $\propto u_{*,\mathrm{w}}^{1}$ to ~~$\propto u_{*,\mathrm{w}}^{3.52}$~~ $\propto u_{*,\mathrm{w}}^{3.0}$ beyond a friction velocity of about $5.8\,\mathrm{cm\,s^{-1}}$. It is a substantial effect, resulting in ~~a more than~~ an about tenfold gas transfer velocity if the water side friction velocity is increased by a factor of two from 6 to $12\,\mathrm{cm\,s^{-1}}$. This substantial increase of the gas transfer velocity is not related to bubble-induced gas transfer at all and thus valid ~~also~~ for all water-side controlled gas tracers independent of the solubility. It is not unexpected that there is no significant difference between seawater and fresh water, because the hydrodynamic conditions do not depend on the salt content of the water and the normalization of the transfer velocity to a Schmidt number of 600 already takes the small change of the kinematic viscosity between seawater and fresh water into account. It is more surprising that there is no significant difference between the Kyoto and SUSTAIN facilities although they differ significantly in lengths (15.7 m versus 24 m) and width (0.8 versus 6 m).

Bubble surface related transfer, $k_{c,600}$: Bubble-induced gas transfer could only be observed after the transition to a much steeper increase of the gas transfer velocity at the surface beyond a friction velocity of $5.8\,\mathrm{cm\,s^{-1}}$. (Fig. 7(b) and (c)). The maximum bubble-induced gas transfer velocity in the limit of low solubility $k_{c,600}$ increases even steeper (Fig. 7(b)).

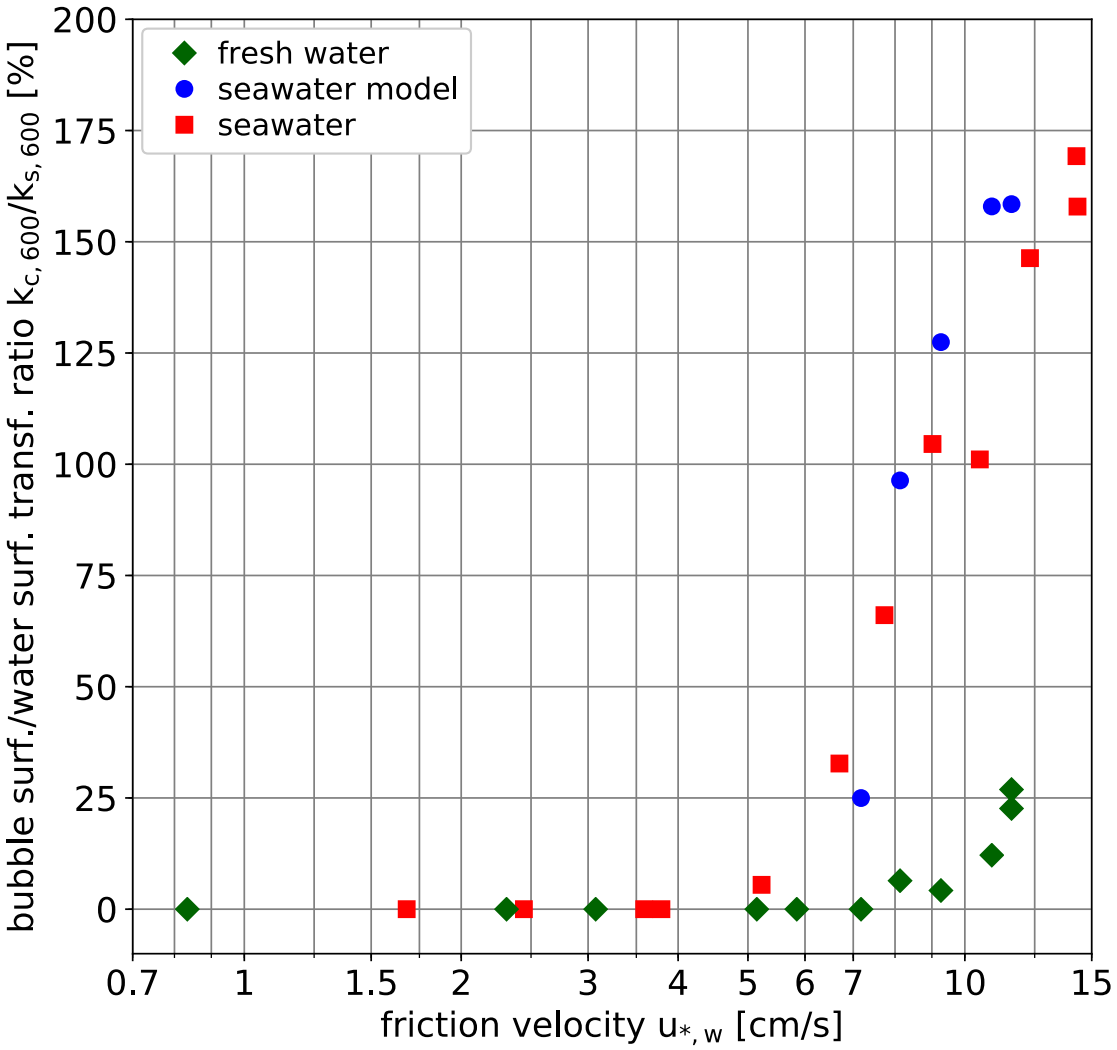

Figure 8. Ratio of $k_{c,600}$ to $k_{s,600}$, i. e., the bubble-induced gas transfer velocity in the limit of low solubility to the gas transfer velocity at the free surface in relation to the friction velocity, given in percent of the gas transfer velocity at the free surface.

For all fresh water conditions studied, bubble-induced gas transfer remains much smaller than the gas transfer at the free water surface. For seawater, however, $k_{c,600}$ is an order of magnitude higher and surpasses $k_{s,600}$ at a friction velocity of about 8 cm s^{-1}. At the highest wind speed it is about 1.7 times larger than at the free surface ~~. This is shown in~~ (Fig. 8~~, where the ratio of $k_{c,600}$ to $k_{s,600}$ is shown as a function of the friction velocity~~). The about tenfold larger bubble-induced gas transfer velocity for seawater than for fresh water in the limit of low solubilities is in good agreement with the measured bubble surface as presented in Sec. 4.2.

Bubble volume flux density related transfer, k_r: ~~In the limit of~~ For high solubility, bubble-induced gas transfer is not significant at all (Fig. 7(c)). It is also not unexpected that there is no significant difference between seawater and fresh water, because in this limit, bubble-induced gas exchange is controlled by the bubble volume flux. It can be expected that the gas volume submerged per breaking wave does not depend on the salt content, because this depends only on the geometry and dynamics of wave breaking.

~~Interestingly, found $k_r = 40$cmh^{-1} in his bubble tank study, a value close to the values at highest wind speeds.~~

Transition solubility α_t: In seawater, however, many more small bubbles are generated, which stay longer in the water and form a significantly larger surface. This is why seawater is much more effective in bubble-induced gas transfer for low solubilities. Therefore also the transition from surface to volume flux controlled bubble-mediated gas transfer is shifted for seawater to lower solubilities (Fig. 7(d)) from fresh water at about 0.4 of values around 0.03.

Within the measurement accuracy, no difference was found between seawater and simulated seawater. Thus not only the absolute values of bubble-induced gas transfer (Fig. 7(b) and (c)) but also the transition solubility is correctly reproduced when using traces of n-Butanol in fresh water to simulate the effect of seawater on bubble generation and its effects on air-sea gas transfer. This greatly simplifies laboratory experiments.

In his bubble tank experiment Mischler (2014) found ~~very~~ similar transition values: for fresh water 0.23 and for saltwater 0.06 at the conditions shown in Fig. 2. The small deviations are not surprising, because in a bubble-tank without wind, where the breaking waves are simulated by a jet, the turbulence in the water certainly is different.

~~The successful partitioning of the gas exchange according to Eq. 11 makes it possible to compute the gas transfer velocity for any gas . This is important because it is now possible to determine the transfer velocity of other important species, which could not be measured with our setup, e.~~

4.5 Comparison with field measurements

4.5.1 Bubble-induced gas transfer

At first glance, the most striking result is the negligible contributions of bubbles to gas transfer up to wind speeds of 30 ~~g., carbon dioxide~~ms^{-1}. There is evidence that bubbles contribute to air-sea gas exchange at much lower wind speeds at the ocean surface. Both Blomquist et al. (2017) and Bell et al. (2017) found significantly higher gas transfer velocities for carbon

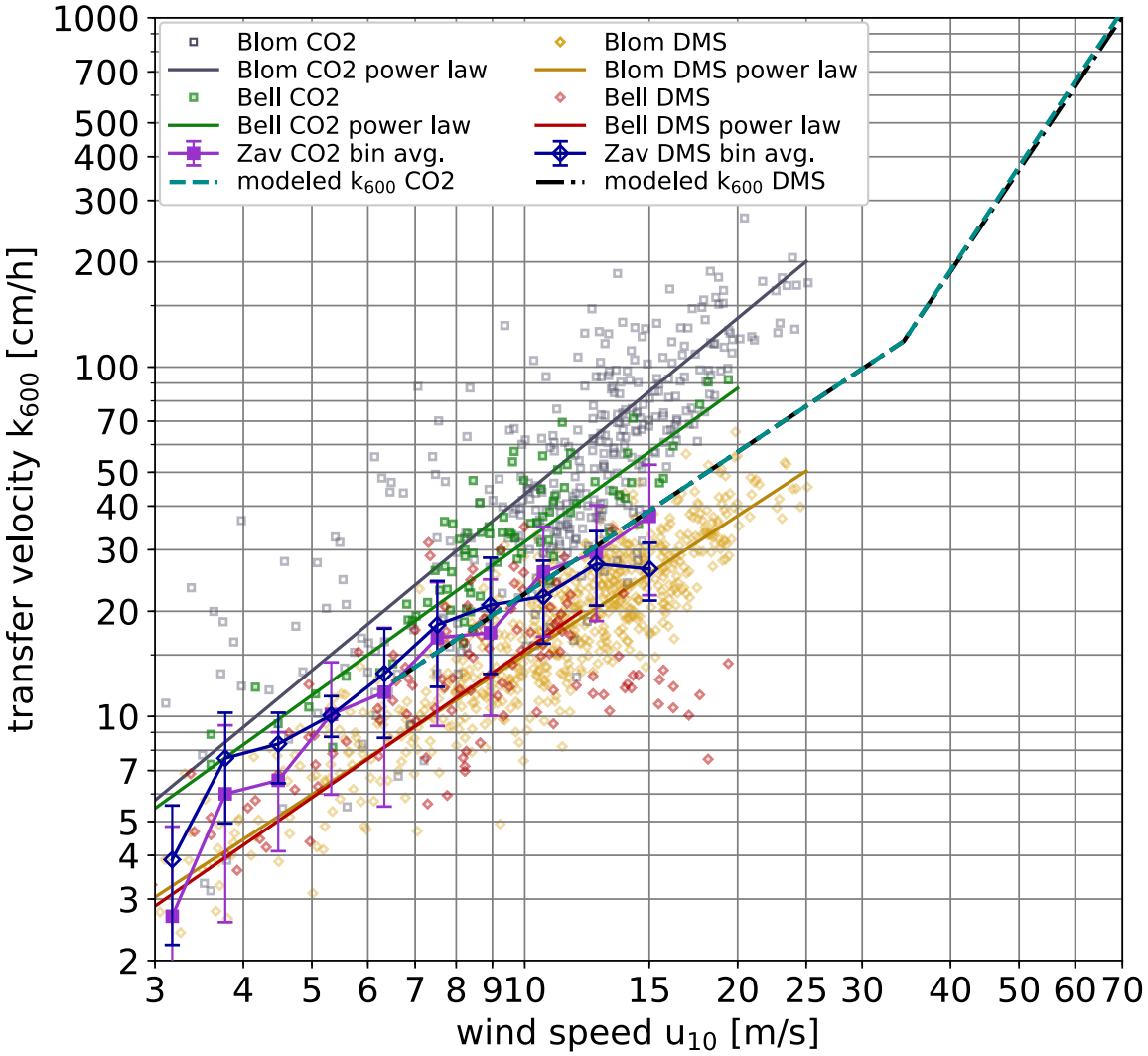

Figure 9. Comparision of DMS and carbon dioxide gas transfer velocities in a double logarithmic representation: eddy covariance measurements from the High Wind Speed Gas Exchange Field Study (HiWinGS) by Blomquist et al. (2017) (Blom) including their $k(u_{10})$-parameterizations. Also shown are the CO_2 and DMS transfer velocities measured by Zavarsky et al. (2018) (Zav) and those reported in Bell et al. (2017) (Bell). For the Bell data, power laws of the form $a\,u_{10}^n$ taken from Brumer et al. (2017) are shown. The output of the model presented in this paper for CO_2 and DMS is also shown.

dioxide than for DMS and attributed this to bubble-induced gas transfer (Fig. 4.5.3). However, doubts remain. First, the field experiment by Zavarsky et al. (2018) did not show a significant difference between DMS and CO_2 gas transfer velocities (Fig. 4.5.3). Secondly, CO_2 gas transfer velocities measured by eddy covariance techniques are generally about a factor of two higher than gas transfer velocities measured with the dual tracer technique using $^3He/SF_6$ (Garbe et al., 2014, Fig. 2.10) when scaled to the same Schmidt number. This should not be the case, because both ^3He and SF_6 have much lower solubilities than CO_2 and consequently should show a higher transfer velocity than CO_2, not a much smaller one.

4.6 ~~Dimethyl sulfide and carbon dioxide~~

4.5.1 Wave age dependency

But even if the bubble-mediated gas transfer is estimated correctly by combined DMS/CO_2 measurements, this does not contradict the laboratory measurements, because of the very different wave ages between linear wind-wave tunnels and the ocean. The bubble surface area measurements reported in Sec. 4.4 and Fig. 5b show indeed larger bubble surface areas with increasing fetch at the same wind speed. In the Heidelberg Aeolotron with infinite fetch, the same bubble surface area occurs at about half the wind speed than in the short-fetch Kyoto facility.

Therefore it appears logical that wave breaking in the ocean could be more intense than in a short-fetch wind-wave tank and thus would start to become significant at considerably lower wind speeds. This is supported by the estimation of air entrainment by breaking waves by Deike et al. (2017). They estimated maximum air entrainment velocities $V_a = k_r$ up to about 50 cm h^{-1}, as we did (Fig. 2c), but already at much lower wind speeds.

However with the current state of knowledge, it is not possible to draw definitive conclusions. As pointed out by Brumer et al. (2017), some field measurements showed a significant wave age dependency others did not. And there are contradictionary theoretical and semiempiric models as the discussion about the findings by (Deike et al., 2017; Deike and Melville, 2018) in the last paragraph of Sec. 2.2 showed.

4.5.2 DMS gas transfer

~~The gas transfer velocities measured for dimethyl sulfide (DMS)deserve some more discussion here, because they partly contradict the results of previous field experiments.~~

~~The~~ One set of eddy covariance measurements ~~of~~ (Bell et al., 2013, 2015) found a decrease of the gas transfer for wind speeds higher than approx. ~~15~~12 m s^{-1}, while all other field measurements do not show this effect (Fig. 10) ~~.~~The measurements presented here do not show such an effect (Fig. 10). On the contrary: beyond a wind speed of about 33 m s^{-1}, the transfer velocity shows the same transition to a much steeper increase as all other tracers used. ~~More recent field measurements do not show a decrease in the DMS transfer velocity . found that the increase in the gas transfer velocity with wind speed becomes less steep at higher wind speeds.~~ Thus the transfer of DMS across the air-water interface in fresh water and seawater is just the same as for all other gases and volatile tracers and theories about an attenuated Henry's law constant for DMS (Vlahos and Monahan, 2009) are most likely not correct.

~~Measured transfer velocities of DMS, scaled to k_{600}, compared to previous field studies. B2013: ; B2015: ; B2017: ; Z2018: .~~

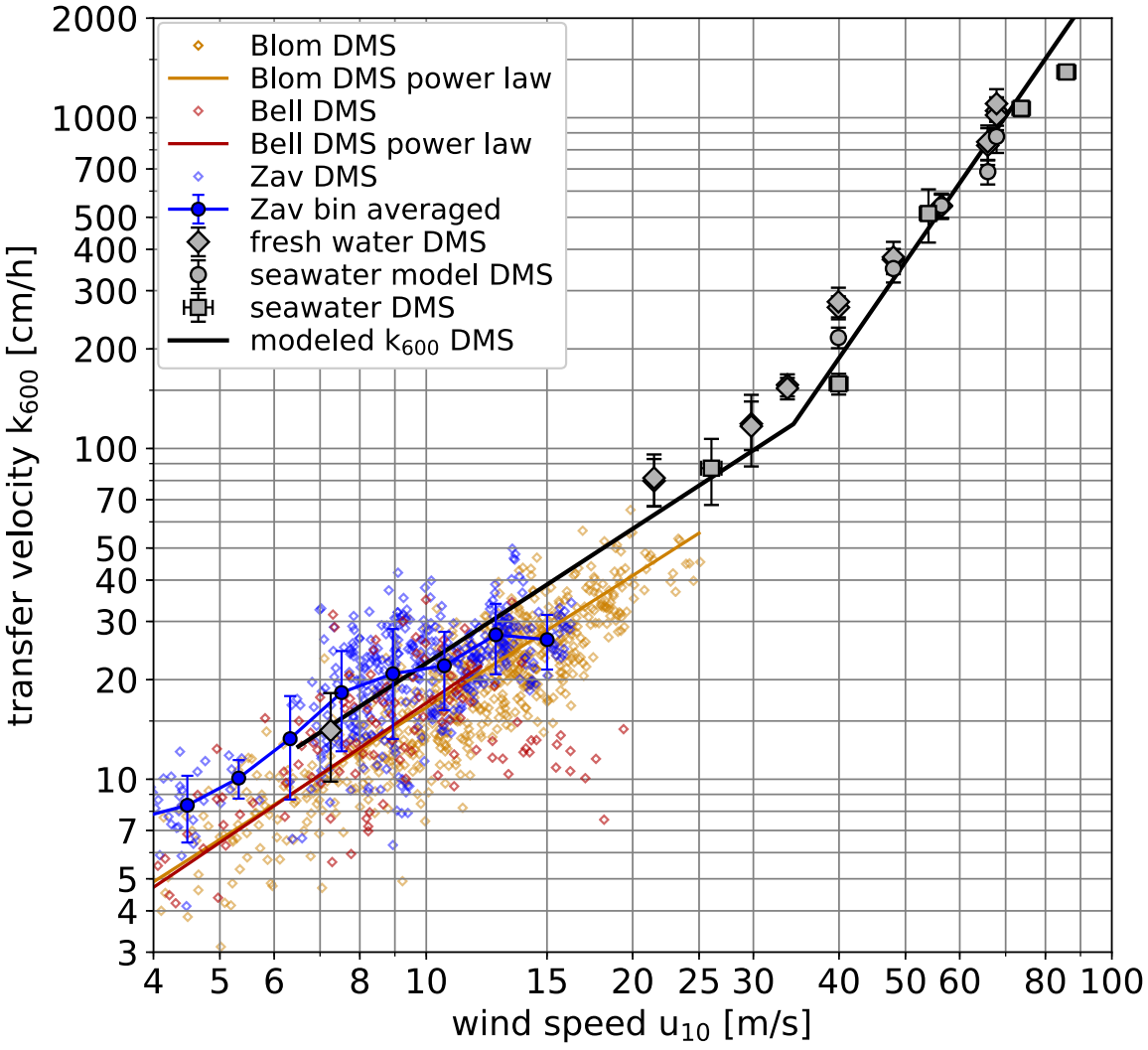

Figure 10. Measured transfer velocities of DMS, scaled to k_{600}, compared to previous field studies. Bell: Bell et al. (2017); Blom: Blomquist et al. (2017); Zav: Zavarsky et al. (2018).

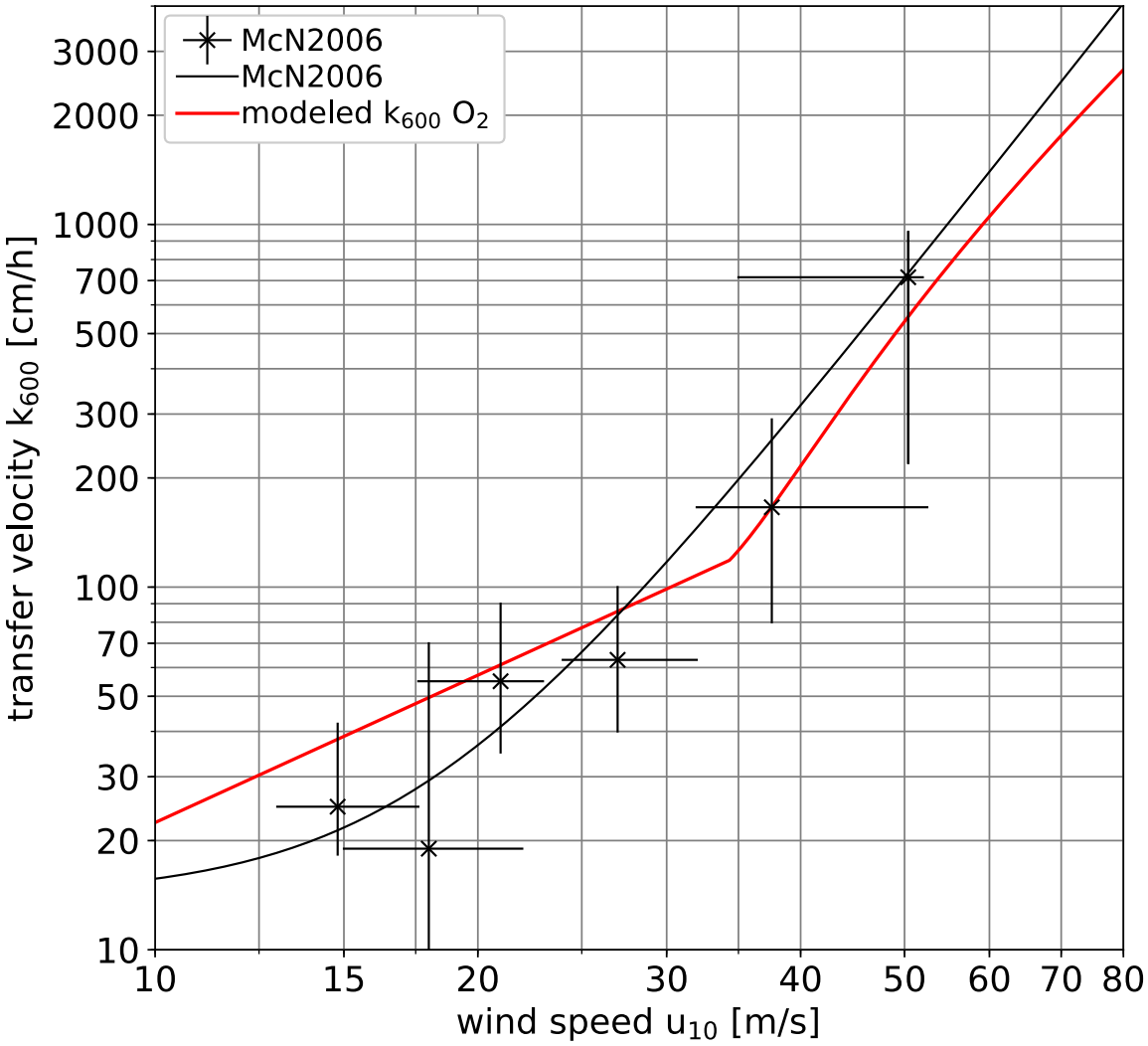

Figure 11. Comparison of oxygen gas transfer velocities inferred from the lab measurements presented in this paper with the field data by McNeil and D'Asaro (2007), both Schmidt number scaled to k_{600}.

~~Because it is well known that parameters other than wind speed influence gas exchange , a direct comparison of field data with laboratory data based on the wind speed alone is not adequate. Therefore, the remaining question is whether it is physically reasonable that in a wind speed range of 12 to 20~~

4.5.3 Very high wind speeds

The most interesting and novel result is the steep increase of the gas transfer velocity beyond 33 m s^{-1} ~~the gas transfer velocity varies by almost a factor of three at the same wind. Currently there is no evidence available from laboratory measurements that would confirm this. The influence of fetch and thus waves on gas transfer has so far only been studied at wind speeds of less than 10ms^{-1} and proved to be only significant at wind speeds lower than 6~~to values exceeding 1000 ~~m~~cm h^{-1}~~. However, recent measurements in the Baltic Sea using active thermography also showed large variations in the gas transfer velocity at wind speeds higher than 10ms^{-1}, which is most likely related to the effect of surfactants .~~

~~Comparision of DMS and carbon dioxide gas transfer velocities in a double logarithmic representation: eddy covariance measurements from the High Wind Speed Gas Exchange Field Study (HiWinGS) (B2017). Also shown are the CO_2 and DMS transfer velocities measured by (Z2018). The output of the model presented in this paper for CO_2 and DMS is also shown.~~

~~There is another striking discrepancy. found significantly higher~~ . In this wind speed range the comparison with only two transfer velocities estimated in a field measurement with oxygen is possible (McNeil and D'Asaro, 2007). The modeled values of the oxygen gas transfer velocities ~~for carbon dioxide than for DMS and attributed this to bubble-induced gas transfer, whereas the measurements presented here do not show any significant bubble-induced gas exchange for both gases in the wind speed range covered by the HiWinGS study and even at much higher wind speeds~~ were calculated according to Eq. 11 and the model equations contained in the supplementary material. It is interesting to see how close our wind-wave tank data are to the field data (Fig. ~~4.5.3). Actually, the figure shows that the transfer velocity for carbon dioxide is an almost constant factor of three higher than that of DMS in the whole~~ 4.6). This clearly means that the mechanisms causing this steep increase in the laboratory in this wind speed range ~~from 3.4 to 25ms^{-1} for the field data set of . It is unlikely that a) already at 3.4ms^{-1} wind speed, the bubble-induced gas exchange increases the transfer velocity of carbon dioxide threefold over DMS and b) that this effect neither increases, nor decreases with wind speed . Also, no such discrepancy between the gas transfer velocities of DMS and CO_2 spanning all wind speeds was found in a similar study by , see Fig. 4.5.3. The laboratory measurements presented here may provide some insight into the cause for this discrepancy.~~ are also relevant for field conditions.

~~Wave breaking in the ocean could be more intense than in a short-fetch~~

4.5.4 From lab to ocean conditions

It is evident that gas transfer cannot be directly transferred from a wind-wave ~~tank and thus also the bubble-induced gas exchange would be stronger and would start to become significant at lower wind speeds. Indeed, the bubble surface area measurements reported in Sec. 4.4 and Fig. 5b show larger bubble surface areas with increasing fetch at the same wind speed. In the Heidelberg Aeolotron with infinite fetch, the same bubble surface area occurs at about half the wind speed than in~~ flume to the ocean. This is just as wrong as using empirical gas transfer - wind speed relations from a collection of field experiments, because parameters other than wind speed also influence gas transfer. This is not just the sea state as discussed above, but also the influence of surface active material at the water surface (Frew, 1997; Cunliffe et al., 2013; Nagel et al., 2019). It is exactly this multitude of parameters influencing air-sea gas transfer, which makes it so difficult to identify and quantify the mechanisms. Here laboratory studies can play an important role. Laboratory measurements are generally much more precise

and accurate than any current field measuring techniques. It is possible to use many more tracers simultaneously. Also, it is easy to perform systematic studies.

There were two serious limitations in the past: The limited wind speeds and low-fetch conditions. The first limitation is already gone with the ~~short-fetch Kyoto facility~~Kyoto High Speed Wind-Wave Facility and the Miami SUSTAIN Facility. The second limitation can be overcome in annular facilities such as the Heidelberg Air-Sea Interaction Facility, the Aeolotron. It is not required to perform perfect replications of ocean conditions. This will not be possible anyways. It is just necessary to describe the findings with physically-based models that cover all important mechanisms and then to adapt the parameters to conditions at the ocean surface.

One may argue that large breaking waves cannot be simulated adequately in wind-wave tunnels. However, ~~even if the fetch effect was larger at the open ocean, bubble-induced gas exchange would become significant only beyond a critical wind speed, which is for sure larger than a calm 3.4ms^{-1}.~~

the basic physical mechanisms seem to be remarkably scale-independent. Air entrainment from breaking waves is a good example for this. Su and Cartmill (1995) measured bubble distributions and void fractions in a 90 m long, 3.36 m deep and 3.66 m wide wave channel with large mechanically generated breaking waves using fresh water and artificial seawater. They found an about tenfold larger bubble surface area in sea water than in fresh water, but no significant change in the void fraction, which agrees well with our findings ~~. This is a strong indication that the fundamental physical mechanisms for bubble-induced gas exchange are not sensitive to the scales from rather short and shallow wind-wave tanks used in this study to longer and deeper wave tanks. Therefore, it is unlikely that the physical mechanisms are different in the ocean, and the transition solubility α_t in the field is expected to be similar to α_t measured in the lab. In seawater it is around 0.03, which results in a reduction of bubble-induced gas transfer of carbon dioxide by a factor of more than 20 in comparison to the low-solubility limit $k_{c,600}$, see Eqns. 8, 9 and Fig. 4.5.3. Consequently, bubble-induced gas transfer is not significant for both carbon dioxide and DMS and therefore cannot be the cause for the different gas transfer velocities reported in~~ in much shallower facilities. In a small-scale tipping bucket experiment, Carey et al. (1993) compared air entrainment in seawater and fresh water and found, as we did in our experiments, that the volume flux of air entrainment is about the same for both water types.

4.6 ~~Comparison with field data at hurricane wind speeds~~

~~Comparison of oxygen gas transfer velocities inferred from the lab measurements presented in this paper with the field data by , both Schmidt number scaled to k_{600}.~~

~~As a final step, Fig. 4.6 shows a comparison of our results with the only available field data set at hurricane wind speeds . The oxygen gas transfer velocities were calculated according to Eq. 11 and the model equations are shown in App. **??**. It is interesting to see how close our wind-wave tank data are to the field data. This does not mean that the laboratory data can simply be extrapolated to the field. This would physically not be correct and in addition, the uncertainties of the field data are too large for such a statement. It does show, however, that wind-wave tank studies do not miss an essential mechanisms compared to ocean conditions.~~

5 Conclusions and outlook

With multi-tracer gas exchange experiments in two high-speed wind-wave tanks it was possible to separate the mechanisms of air-sea gas transfer into its different components~~.~~, transfer across the free water surface, transfer across closed bubble surfaces and transfer associated with the bubble volume flux density.

In the short-fetch tanks, a steep increase of the transfer velocity across the free surface was found beyond wind speeds of 33 $m\,s^{-1}$ (friction velocity in water 5.8 $cm\,s^{-1}$) increasing the transfer velocity corrected to a Schmidt number of 600 from 110 $cm\,h^{-1}$ to a maximum measured value of about 1600 $cm\,h^{-1}$. This part of the gas transfer is the same in fresh water and seawater.

It is obvious that a new regime is established at wind speeds beyond 33 $m\,s^{-1}$, which is governed by the intense turbulent mixing and permanent rapid disruption of the surface. The detailed mechanisms causing the steep increase of the gas transfer velocity at high wind speeds are still unclear and require further investigations. Because this effect is clearly not caused by gas transfer through closed bubble surfaces, it can be explained as either significantly enhanced turbulence at the water surface, or a significantly enlarged surface area for the exchange processes, or a combination of both. Many processes must be considered at highest wind speeds, including the generation of steep small-scale surface waves, the fragmentation of wave crests where the bag-breakup mechanism is dominant (Troitskaya et al., 2017), the effects of high-speed spray and spume droplets plunging into the water surface again and the effects of bursting bubbles. The finding of the relatively low transfer velocity for He at the highest wind speed (Sec. 4.4) is a first indication that rapid surface fragmentation processes play an important role, but further studies are required. It can be expected that this new regime with a steep increase of the gas transfer velocity for all tracers independent of solubility exits with the same type of mechanisms at sea. This regime has still to be explored at sea.

~~In fresh water bubble-induced gas transfer does not play a significant role at all . Even at the highest wind speed and in the high limit for low soluble gases it is just about 25of the gas transfer across the free water surface. In seawater~~ Bubble-mediated gas transfer might differ between the lab measurements presented here and field measurements, because of the wave age or fetch dependency. As has been discussed in detail in Sec. 4.5.1, the wave age dependency of air-sea gas transfer is not well known and urgently requires more detailed investigations. Only then will it be possible to quantify the bubbles' influence on air-sea gas exchange in the field and, more specifically, to which extend an important tracer such as carbon dioxide will be influenced by bubble-induced ~~gas transfer is about an order of magnitude larger and becomes an important contribution for gases with low solubility. At the highest measured wind speed of 80ms^{-1} it is about 1.7 times larger than the~~ gas ~~transfer at the free water surface. For moderately soluble gases such as the widely studied tracers carbon dioxide and DMS, bubble-induced gas~~ transfer~~is still not a significant process because transition solubility α_t from the surface-related to volume flux related gas transfer was found to be at a quite low value of around 0.03. Therefore, DMS and carbon dioxide should show the same gas exchange velocities at all~~ . In the laboratory experiments reported here, bubbles did not significantly contribute to CO_2 gas transfer even at the highest wind speeds.

~~Bubble measurements in two additional facilities, especially in the annular Heidelberg Aeolotron, suggest that the steep increase of bubble concentrations is likely shifted to lower wind speeds at infinite fetch. This means that the high wind speed~~

regime could start at lower wind speeds for larger fetches. However, the effect cannot be too large because the short-fetch wind-wave tank results agree surprisingly well with the only field data set at hurricane wind speeds by .

In field experiments it remains very difficult to reveal the mechanisms of air-sea gas transfer because there are not enough tracers available simultaneously to span the necessary wide range of tracer solubility and diffusivity . Systematic field studies addressing the mechanisms are therefore hardly possible. and because systematic studies scanning all relevant environmental conditions are very demanding and time consuming. As this study has shown, systematic and well-designed wind-wave tank experiments have more potential to reveal the mechanisms of the gas transfer processes. This opens also the opportunity to predict transfer velocities under field conditions.

However, the most serious limitation is the short fetch of the linear laboratory facilities. High Especially future high wind speed gas transfer studies in the annular Heidelberg Aeolotron with infinite fetch have the potential to close narrow the "fetch gap"" between the laboratory and the field.

Data availability. All measured data reported and discussed in this paper will be published on the free and open digital archive zenodo within the small-scale air-sea interaction community, https://zenodo.org/communities/asi once this paper has been accepted for publication. All third party data sets used are cited in the text.

6 Model equations

All $u_{*,w}$ in cms^{-1}, all k in cmh^{-1}.

$k_{s,600}$ for fresh water and seawater:

$$k_{s,600} = 8.225^{-1} u_{*,w} 600^{-1/2} \text{if} 0.75 < u_{*,w} < 5.8 \; 0.214 u_{*,w}^{3.52} \text{if} 5.8 \leq u_{*,w} < 13.$$

$k_{c,600}$ for seawater:

$$k_{c,600} = 0 \text{if} 0.75 < u_{*,w} < 5.8 \; 4.01(u_{*,w} - 5.8)^{2.20} \text{if} 5.8 \leq u_{*,w} < 13.$$

$k_{c,600}$ for fresh water:

$$k_{c,600} = 0 \text{if} 0.75 < u_{*,w} < 5.8 \; 51.3(u_{*,w} - 5.8)^{2.07} \text{if} 5.8 \leq u_{*,w} < 13.$$

k_r for fresh water and seawater:

$$k_r = 0 \text{if} 0.75 < u_{*,w} < 5.8 \; 1.19(u_{*,w} - 5.8)^{2.044} \text{if} 5.8 \leq u_{*,w} < 13.$$

Author contributions. KEK planned the experiments, performed the measurements, evaluated the data and prepared all figures. BJ contributed to planning of the experiments, worked on the bubble model and drafted the main conclusions. KEK and BJ contributed equally to

writing the paper. NT and AS performed the wind speed measurements and contributed to the section about the wind speed measurements in the Kyoto and SUSTAIN experiments, respectively.

Competing interests. None

Acknowledgements. The authors gratefully acknowledge the significant help of many people. Satoru Komori and Brian Haus kindly allowed us to run their wind-wave tanks at the most extreme wind speeds. ~~Wind data in Miami was provided by Andrew Smith.~~ Wolfgang Mischler and Angelika Klein contributed to the measurements in Kyoto. Sonja Friman and Jan Bug participated in the measurements in Miami. ~~Naohisa Takagaki, Andrew Smith,~~ Michael Rebozo, Cedric Guigand, Neil Williams, Nathan Laxague, David Ortiz-Suslow and Brian Haus helped with the set-up of our equipment and provided invaluable logistical support. We gratefully acknowledge partial financial support of this research by the German Science Foundation (DFG), grants JA 395/17-1&2 "Air-Sea Gas Exchange at High Wind Speeds".

References

Abraham, M. H. and Matteoli, E.: The temperature variation of the hydrophobic effect, J. Chem. Soc., Faraday Trans. 1, 84, 1985–2000, https://doi.org/10.1039/F19888401985, http://dx.doi.org/10.1039/F19888401985, 1988.

Alves, S., Orvalho, S., and Vasconcelos, J.: Effect of bubble contamination on rise velocity and mass transfer, Chemical Engineering Science, 60, 1–9, http://www.sciencedirect.com/science/article/B6TFK-4DB5576-6/2/a8d543a276dca02cf7923e7bfa34c30e, 2005.

Andreas, E. L. and Emanuel, K. A.: Effects of Sea Spray on Tropical Cyclone Intensity., Journal of Atmospheric Sciences, 58, 3741–3751, https://doi.org/10.1175/1520-0469(2001)058<3741:EOSSOT>2.0.CO;2, 2001.

Andreas, E. L., Vlahos, P., and Monahan, E. C.: Spray-mediated air-sea gas exchange: the governing time scales, J. Mar. Sci. Eng., 5, 60, https://doi.org/10.3390/jmse5040060, 2017.

Asher, W. E., Higgins, B. J., Karle, L. M., Farley, P. J., Sherwood, C. R., Gardiner, W. W., Wanninkhof, R., Chen, H., Lantry, T., Steckley, M., Monahan, E. C., Wang, Q., and Smith, P. M.: Measurement of gas transfer, whitecap coverage, and brightness temperature in a surf pool: an overview of WABEX-93, in: Air-Water Gas Transfer, Selected Papers, 3rd Intern. Symp. on Air-Water Gas Transfer, edited by Jähne, B. and Monahan, E., pp. 205–216, AEON, Hanau, https://doi.org/10.5281/zenodo.10571, 1995.

Asher, W. E., Karle, L. M., Higgins, B. J., Farley, P. J., Monahan, E. C., and Leifer, I. S.: The influence of bubble plumes on air-seawater gas transfer velocities, J. Geophys. Res., 101, 12 027–12 041, https://doi.org/10.1029/96JC00121, 1996.

Bell, T. G., Bruyn, W. D., Miller, S. D., Ward, B., Christensen, K. H., and Saltzman, E. S.: Air-sea dimethylsulfide (DMS) gas transfer in the North Atlantic: evidence for limited interfacial gas exchange at high wind speed, Atmos. Chem. Phys., 13, 11 073–11 087, https://doi.org/10.5194/acp-13-11073-2013, 2013.

Bell, T. G., Bruyn, W. D., Marandino, C. A., Miller, S. D., Law, C. S., Smith, M. J., and Saltzman, E. S.: Dimethylsulfide gas transfer coefficients from algal blooms in the Southern Ocean, Atmos. Chem. Phys., 15, 1783–1794, https://doi.org/10.5194/acp-15-1783-2015, 2015.

Bell, T. G., Landwehr, S., Miller, S. D., de Bruyn, W. J., Callaghan, A. H., Scanlon, B., Ward, B., Yang, M., and Saltzman, E. S.: Estimation of bubble-mediated air–sea gas exchange from concurrent DMS and CO_2 transfer velocities at intermediate–high wind speeds, Atmospheric Chemistry and Physics, 17, 9019–9033, https://doi.org/10.5194/acp-17-9019-2017, https://www.atmos-chem-phys.net/17/9019/2017/, 2017.

Blomquist, B. W., Brumer, S. E., Fairall, C. W., Huebert, B. J., Zappa, C. J., Brooks, I. M., Yang, M., Bariteau, L., Prytherch, J., Hare, J. E., Czerski, H., Matei, A., and Pascal, R. W.: Wind speed and sea state dependencies of air-sea gas transfer: results from the high wind speed gas exchange study (HiWinGS), J. Geophys. Res., 122, 8034–8062, https://doi.org/10.1002/2017JC013181, 2017.

Brumer, S. E., Zappa, C. J., Blomquist, B. W., Fairall, C. W., Cifuentes-Lorenzen, A., Edson, J. B., Brooks, I. M., and Huebert, B. J.: Wave-related Reynolds number parameterizations of CO2 and DMS transfer velocities, Geophys. Res. Lett., 44, 9865–9875, https://doi.org/10.1002/2017GL074979, 2017.

Carey, W. M., Fitzgerald, J. W., Monahan, E. C., and Wang, Q.: Measurments of the sound produced by a tipping trough with fresh and salt water, J. Acoust. Soc. Am., 93, 3178–3192, https://doi.org/10.1121/1.405702, 1993.

Cunliffe, M., Engel, A., Frka, S., Gasparovic, B., Guitart, C., Murrell, J. C., Salter, M., Stolle, C., Upstill-Goddard, R., and Wurl, O.: Sea surface microlayers: A unified physicochemical and biological perspective of the air-ocean interface, Prog. Oceanog., 109, 104–116, https://doi.org/10.1016/j.pocean.2012.08.004, 2013.

Deike, L. and Melville, W. K.: Gas transfer by breaking waves, Geophys. Res. Lett., 45, 10 482–10 492, https://doi.org/10.1029/2018GL078758, 2018.

Deike, L., Lenain, L., and Melville, W. K.: Air entrainment by breaking waves, Geophys. Res. Lett., 44, 3779–3787, https://doi.org/10.1002/2017GL072883, 2017.

Donelan, M., Haus, B., Reul, N., Plant, W., Stiassnie, M., Graber, H., Brown, O., and Saltzman, E.: On the limiting aerodynamic roughness of the ocean in very strong winds, Geophys. Res. Lett., 31, https://doi.org/10.1029/2004GL019460, 2004.

Donelan, M. A.: On the decrease of the oceanic drag coefficient in high winds, J. Geophys. Res., 123, 1485–1501, https://doi.org/10.1002/2017JC013394, 2018.

Fenclová, D., Blahut, A., Vrbka, P., Dohnal, V., and Böhme, A.: Temperature dependence of limiting activity coefficients, Henry's law constants, and related infinite dilution properties of C4–C6 isomeric n-alkyl ethanoates/ethyl n-alkanoates in water. Measurement, critical compilation, correlation, and recommended data, Fluid Phase Equilibria, 375, 347 – 359, https://doi.org/https://doi.org/10.1016/j.fluid.2014.05.023, http://www.sciencedirect.com/science/article/pii/S0378381214003148, 2014.

Flothow, L.: Bubble Characteristics from Breaking Waves in Fresh Water and Simulated Seawater, Master's thesis, Institut für Umweltphysik, Universität Heidelberg, Germany, https://doi.org/10.11588/heidok.00023754, 2017.

Frew, N. M.: The role of organic films in air-aea gas exchange, in: The Sea Surface and Global Change, edited by Liss, P. S. and Duce, R. A., pp. 121–171, Cambridge University Press, Cambridge,UK, https://doi.org/10.1017/CBO9780511525025.006, 5, 1997.

Garbe, C. S., Rutgersson, A., Boutin, J., Delille, B., Fairall, C. W., Gruber, N., Hare, J., Ho, D., Johnson, M., de Leeuw, G., Nightingale, P., Pettersson, H., Piskozub, J., Sahlee, E., Tsai, W., Ward, B., Woolf, D. K., and Zappa, C.: Transfer across the air-sea interface, in: Ocean-Atmosphere Interactions of Gases and Particles, edited by Liss, P. S. and Johnson, M. T., pp. 55–112, Springer, https://doi.org/10.1007/978-3-642-25643-1_2, 2014.

Goddijn-Murphy, L., Woolf, D. K., Callaghan, A. H., Nightingale, P. D., and Shutler, J. D.: A reconciliation of empirical and mechanistic models of the air-sea gas transfer velocity, J. Geophys. Res., 121, 818–835, https://doi.org/10.1002/2015JC011096, 2016.

Hiatt, M. H.: Determination of Henry?s Law Constants Using Internal Standards with Benchmark Values, Journal of Chemical & Engineering Data, 58, 902–908, https://doi.org/10.1021/je3010535, 2013.

Iwano, K., Takagaki, N., Kurose, R., and Komori, S.: Mass transfer velocity across the breaking air-water interface at extremely high wind speeds, Tellus B, 65, 21 341, https://doi.org/10.3402/tellusb.v65i0.21341, 2013.

Iwano, K., Takagaki, N., Kurose, R., and Komori, S.: Erratum: Mass transfer velocity across the breaking air-water interface at extremely high wind speeds, Tellus B, 66, 25 233, https://doi.org/10.3402/tellusb.v66.25233, 2014.

Jeong, D., Haus, B. K., and Donelan, M. A.: Enthalpy Transfer across the Air–Water Interface in High Winds Including Spray, Journal of the Atmospheric Sciences, 69, 2733–2748, https://doi.org/10.1175/JAS-D-11-0260.1, 2012.

Jähne, B.: Air-Sea Gas Exchange, in: Encyclopedia of Ocean Sciences, edited by Cochran, J. K., Bokuniewicz, H. J., and Yager, P. L., vol. 6, pp. 1–13, Academic Press, 3 edn., https://doi.org/10.1016/B978-0-12-409548-9.11613-6, 2019.

Jähne, B. and Geißler, P.: Depth from focus with one image, in: Proc. Conference on Computer Vision and Pattern Recognition (CVPR '94), Seattle, 20.-23. June 1994, pp. 713–717, https://doi.org/10.1109/CVPR.1994.323885, 1994.

Jähne, B., Wais, T., and Barabas, M.: A new optical bubble measuring device; a simple model for bubble contribution to gas exchange, in: Gas transfer at water surfaces, edited by Brutsaert, W. and Jirka, G. H., pp. 237–246, Reidel, Hingham, MA, https://doi.org/10.1007/978-94-017-1660-4_22, 1984.

Jähne, B., Heinz, G., and Dietrich, W.: Measurement of the diffusion coefficients of sparingly soluble gases in water, J. Geophys. Res., 92, 10,767–10,776, https://doi.org/10.1029/JC092iC10p10767, 1987.

Jähne, B., Libner, P., Fischer, R., Billen, T., and Plate, E. J.: Investigating the transfer process across the free aqueous boundary layer by the controlled flux method, Tellus, 41B, 177–195, https://doi.org/10.3402/tellusb.v41i2.15068, 1989.

Kestin, J., Sokolov, M., and Wakeham, W. A.: Viscosity of Liquid Water in the Range - 8^{o}C to 150^{o}C, J. Phys. Chem. Ref. Data, 7, 941–948, https://doi.org/10.1063/1.555581, 1978.

King, D. B. and Saltzman, E. S.: Measurement of the diffusion coefficient of sulfur hexafluoride in water, J. Geophys. Res., 100, 7083–7088, https://doi.org/10.1029/94JC03313, 1995.

Komori, S., Iwano, K., Takagaki, N., Onishi, R., Kurose, R., Takahashi, K., and Suzuki, N.: Laboratory Measurements of Heat Transfer and Drag Coefficients at Extremely High Wind Speeds, Journal of Physical Oceanography, 48, 959–974, https://doi.org/10.1175/JPO-D-17-0243.1, 2018.

Krall, K. E. and Jähne, B.: First laboratory study of air-sea gas exchange at hurricane wind speeds, Ocean Sci., 10, 257–265, https://doi.org/10.5194/os-10-257-2014, 2014.

Leifer, I. and De Leeuw, G.: Bubble mesurements in breaking-wave generated bubble plumes during the LUMINY wind-wave experiment, in: Gas Transfer at Water Surfaces, edited by Donelan, M. A., Drennan, W. M., Saltzman, E. S., and Wanninkhof, R., vol. 127 of *Geophysical Monograph*, pp. 303–309, https://doi.org/10.1029/GM127p0303, 2002.

Liss, P. S. and Slater, P. G.: Flux of gases across the air-sea interface, Nature, 247, 181–184, https://doi.org/10.1038/247181a0, 1974.

Maaßen, S.: Experimentelle Bestimmung und Korrelierung von Verteilungskoeffizienten in verdünnten Lösungen, Ph.D. thesis, 1995.

Maiß, M.: Modelluntersuchung zum Einfluss von Blasen auf den Gasaustausch zwischen Atmosphäre und Meer, Diplomarbeit, Institut für Umweltphysik, Fakultät für Physik und Astronomie, Univ. Heidelberg, https://doi.org/10.5281/zenodo.15415, 1986.

McNeil, C. and D'Asaro, E.: Parameterization of air sea gas fluxes at extreme wind speeds, J. Marine Syst., 66, 110–121, https://doi.org/10.1016/j.jmarsys.2006.05.013, 2007.

Memery, L. and Merlivat, L.: Modelling of gas flux through bubbles at the air-water interface, Tellus B, 37B, 272–285, https://doi.org/10.1111/j.1600-0889.1985.tb00075.x, 1985.

Merlivat, L. and Memery, L.: Gas exchange across an air-water interface: experimental results and modeling of bubble contribution to transfer, J. Geophys. Res., 88, 707–724, https://doi.org/10.1029/JC088iC01p00707, 1983.

Mestayer, P. and Lefauconnier, C.: Spray droplet generation, transport, and evaporation in a wind wave tunnel during the humidity exchange over the sea experiments in the simulation tunnel, J. Geophys. Res., 93, 572–586, https://doi.org/10.1029/JC093iC01p00572, 1988.

Mischler, W.: Systematic Measurements of Bubble Induced Gas Exchange for Trace Gases with Low Solubilities, Dissertation, Institut für Umweltphysik, Fakultät für Physik und Astronomie, Univ. Heidelberg, https://doi.org/10.11588/heidok.00017720, 2014.

Mischler, W. and Jähne, B.: Optical measurements of bubbles and spray in wind/water facilities at high wind speeds, in: 12th International Triennial Conference on Liquid Atomization and Spray Systems 2012, Heidelberg (ICLASS 2012), https://doi.org/10.5281/zenodo.10957, 2012.

Monahan, E. C. and Spillane, M. C.: The role of oceanic whitecaps in air-sea gas exchange, in: Gas transfer at water surfaces, edited by Brutsaert, W. and Jirka, G. H., pp. 495–503, Reidel, Hingham, MA, https://doi.org/10.1007/978-94-017-1660-4_45, 1984.

Nagel, L., Krall, K. E., and Jähne, B.: Measurement of air-sea gas transfer velocities in the Baltic Sea, Ocean Sci., 15, 235–247, https://doi.org/10.5194/os-15-235-2019, 2019.

Patro, R., Leifer, I., and Bowyer, P.: Better bubble process modeling: improved bubble hydrodynamics parameterization, in: Gas Transfer at Water Surfaces, edited by Donelan, M. A., Drennan, W. M., Saltzman, E. S., and Wanninkhof, R., vol. 127 of *Geophysical Monograph*, pp. 315–320, https://doi.org/10.1029/GM127p0315, 2002.

Powell, M. D., Vickery, P. J., and Reinhold, T. A.: Reduced drag coefficient for high wind speeds in tropical cyclones, Nature, 422, 279–283, https://doi.org/10.1038/nature01481, 2003.

Reichl, A.: Messung und Korrelierung von Gaslöslichkeiten halogenierter Kohlenwasserstoffe, Ph.D. thesis, 1995.

Sander, R.: Compilation of Henry's law constants (version 4.0) for water as solvent, Atmos. Chem. Phys., 15, 4399–4981, https://doi.org/10.5194/acp-15-4399-2015, 2015.

Sander, S. P., Abbatt, J., Barker, J. R., Burkholder, J. B., Friedl, R. R., Golden, D. M., Huie, R. E., Kolb, C. E., Kurylo, M. J., Moortgat, G. K., Orkin, V. L., and Wine, P. H.: Chemical Kinetics and Photochemical Data for Use in Atmospheric Studies, Evaluation No. 17, http://jpldataeval.jpl.nasa.gov, 2011.

Soloviev, A. and Lukas, R.: Effects of bubbles and sea spray on air-sea exchange in hurricane conditions, Boundary-Layer Meteorology, 136, 365–376, https://doi.org/10.1007/s10546-010-9505-0, 2010.

Su, M.-Y. and Cartmill, J.: Effects of salinity on breaking wave generated void fraction and bubble size spectra, in: Air-Water Gas Transfer, Selected Papers, 3rd Intern. Symp. on Air-Water Gas Transfer, edited by Jähne, B. and Monahan, E., pp. 305–311, AEON, Hanau, https://doi.org/10.5281/zenodo.10571, 1995.

Takagaki, N., Komori, S., Suzuki, N., Iwano, K., Kuramoto, T., Shimada, S., Kurose, R., and Takahashi, K.: Strong correlation between the drag coefficient and the shape of the wind sea spectrum over a broad range of wind speeds, Geophys. Res. Lett., 39, https://doi.org/10.1029/2012GL053988, 2012.

Toba, Y.: Local balance in the air-sea boundary processes I. On the growth process of wind waves, Journal of the Oceanographical Society of Japan, 28, 109–121, https://doi.org/10.1007/BF02109772, 1972.

Troitskaya, Y., Kandaurov, A., Ermakova, O., Kozlov, D., Sergeev, D., and Zilitinkevich, S.: Bag-breakup fragmentation as the dominant mechanism of sea-spray production in high winds, Sci. Rep., 7, 1614, https://doi.org/10.1038/s41598-017-01673-9, 2017.

Vlahos, P. and Monahan, E. C.: A generalized model for the air-sea transfer of dimethyl sulfide at high wind speeds, Geophys. Res. Lett., 36, 0094–8276, https://doi.org/10.1029/2009GL040695, 2009.

Wanninkhof, R., Asher, W. E., Ho, D. T., Sweeney, C., and McGillis, W. R.: Advances in quantifying air-sea gas exchange and environmental forcing, Annu. Rev. Marine Sci., 1, 213–244, https://doi.org/10.1146/annurev.marine.010908.163742, 2009.

Warneck, P. and Williams, J.: The Atmospheric Chemist's Companion, Numerical Data for Use in the Atmospheric Sciences, Springer, Dordrecht, https://doi.org/10.1007/978-94-007-2275-0, 2012.

Woolf, D., Leifer, I., Nightingale, P., Rhee, T., Bowyer, P., Caulliez, G., de Leeuw, G., Larsen, S., Liddicoat, M., Baker, J., and Andreae, M.: Modelling of bubble-mediated gas transfer: Fundamental principles and a laboratory test, J. Marine Syst., 66, 71–91, https://doi.org/10.1016/j.jmarsys.2006.02.011, 2007.

Woolf, D. K. and Thorpe, S. A.: Bubbles and the air-sea exchange of gases in near-saturation conditions, J. Marine Res., 49, 435–466, https://doi.org/10.1357/002224091784995765, 1991.

Yaws, C.: Transport Properties of Chemicals and Hydrocarbons, Elsevier Science, https://doi.org/10.1016/C2013-0-12615-3, https://books.google.de/books?id=uw10AwAAQBAJ, 2014.

Zavarsky, A., Goddijn-Murphy, L., Steinhoff, T., and Marandino, C. A.: Bubble-Mediated Gas Transfer and Gas Transfer Suppression of DMS and CO2, Journal of Geophysical Research: Atmospheres, 123, 6624–6647, https://doi.org/10.1029/2017JD028071, https://agupubs.onlinelibrary.wiley.com/doi/abs/10.1029/2017JD028071, 2018.

Zheng, J., Fei, J., Du, T., Wang, Y., Cui, X., Huang, X., and Li, Q.: Effect of sea spray on the numerical simulation of super typhoon 'Ewiniar', Journal of Ocean University of China, 7, 362–372, https://doi.org/10.1007/s11802-008-0362-0, https://doi.org/10.1007/s11802-008-0362-0, 2008.